CHARGED PION PHOTOPRODUCTION FROM DEUTERIUM FOR PHOTON ENERGIES OF 500 TO 1000 MEV

Thesis by

Walter D. Wales

In Partial Fulfillment of the Requirements

For the Degree of

Doctor of Philosophy

California Institute of Technology

Pasadena, California

1960

ACKNOWLEDGEMENTS

Dr. Robert L. Walker supervised this experiment. His advice and discussions were very helpful in its performance and in the subsequent analysis. The experimental work on the Caltech Synchrotron was performed jointly with Mr. Gerry Neugebauer, who also collaborated in the analysis.

Dr. Matthew Sands made many helpful suggestions during the course of the experiment and its analysis. His advice and guidance during the writer's graduate residence are gratefully acknowledged. The support and interest of Dr. Robert F. Bacher are appreciated.

Mr. James H. Boyden and Mr. Charles W. Peck provided active assistance during the experimental phases of this project. The liquid deuterium target was maintained by Mr. Earle B. Emery. Mr. Lawrence B. Loucks, Mr. Alfred A. Neubeiser, Mr. Lucien Luke and the synchrotron crew were of continuous assistance.

Financial support was provided in part by the United States Atomic Energy Commission.

ABSTRACT

The yields of charged pions photoproduced from deuterium have been measured at several pion angles for photon energies between 500 and 1000 Mev. Pions produced in a liquid deuterium target by the photon beam of the Caltech electron synchrotron were deflected by a wedge-shaped magnet into a set of scintillation counters.

The ratio of the differential cross-sections for the production of negative and positive pions has been determined. This ratio varies from 0.4 to 2.8. The ratio decreases at high photon energies for all pion angles, reaching a value near 0.5 for all pion center-of-mass angles less than 150°.

The absolute values of the differential cross-sections for the photoproduction of positive pions from deuterium have been determined and compared with the corresponding cross-sections measured previously from hydrogen. The ratio of these cross-sections averages about 0.95. The difference between the positive pion cross-sections from deuterium and those from hydrogen seems compatible with measurements which have been made of the elastic photodisintegration of the deuteron.

TABLE OF CONTENTS

LIST OF FIGURES

LIST OF TABLES

I. INTRODUCTION

The investigation of the nature of the nucleon is one of the major problems of high energy nuclear physics. One of the experimental methods of attacking this problem is to explore the interactions of the nucleon with other particles, in the hope that such an exploration will provide some clue to the nature of the interaction and of the nucleon structure. Since pions are assumed to be the carriers of the nuclear forces, it is not surprising that a great deal of effort has been spent in the study of the pion-nucleon interactions.

The photoproduction of pions from nucleons is one of several methods which have been used to investigate the pion-nucleon interaction. Of the four interactions in which single pions are produced by photons,

$$\gamma + p \rightarrow \pi^{+} + n$$
$$\gamma + p \rightarrow \pi^{o} + p$$
$$\gamma + n \rightarrow \pi^{-} + p$$
$$\gamma + n \rightarrow \pi^{o} + n,$$

the first two have been studied most extensively for photon energies of less than 1000 Mev (1-4). Since there are no free neutrons available, the direct observation of either of the last two interactions is not possible. The behavior of these interactions can be determined, however, by a suitable treatment of the data obtained from pion photoproduction from deuterium.

Neutral pion photoproduction from the neutron may be studied by subtracting the neutral pion yields from hydrogen from

the corresponding yields from deuterium (5). Charged pion photoproduction from the neutron is usually studied by examining the ratio of yields of negative and positive pions produced from deuterium. The cross-sections for the photoproduction of charged pions from the neutron may be determined by combining this ratio with the cross-sections for the photoproduction of charged pions from hydrogen. Although the deuteron structure may modify the interaction, those structure effects which affect the positive and negative pion production in the same manner will not affect the measured ratio.

Previous measurements of the π^-/π^+* ratio from deuterium (6) showed that this ratio was about 1.4 for all pion angles near threshhold. At forward angles in the center-of-mass system, the ratio decreased monotonically from threshhold to a value of nearly 1.0 at a photon energy of 450 Mev. At backward pion angles, the ratio increased from threshhold, reaching a value near 1.7 at a photon energy of 450 Mev.

The present experiment was designed to extend the measurements of the π^-/π^+ ratio from deuterium into the photon energy interval from 500 to 1000 Mev. This would complement recent work done on the charged pion photoproduction from hydrogen (4).

---

*The following notation will be used throughout this paper:

$d\sigma/d\Omega^*$ = differential cross-section in center-of-mass system

σ = total cross-section

$\frac{\pi^-}{\pi^+} = \frac{d\sigma^-/d\Omega^*}{d\sigma^+/d\Omega^*}$

The measurement of the ratio of charged pion photoproduction from deuterium also avoided many of the errors due to the absolute calibration of the experimental equipment, which would affect absolute cross-section measurements.

The bremsstrahlung beam of the California Institute of Technology electron synchrotron was passed through a liquid deuterium target. Charged particles produced in the deuterium were detected by a magnetic spectrometer. Those events due to pions were electronically differentiated from those due to other charged particles of the same momentum. The shift from positive to negative pion detection was made by reversing the field of the spectrometer magnet.

The π^-/π^+ ratios which were obtained from this experiment are in agreement, at those places where a comparison can be made, with the results of experiments at lower energies. The ratio shows considerable variation for photon energies between 500 and 1000 Mev. The ratio decreases with increasing photon energy for pion center-of-mass angles less than 120°, reaching a value near 0.5 at 900 Mev. There is some indication that the ratio begins to increase at 900 Mev, but the evidence is contradictory. The ratio increases with energy for pion center-of-mass angles of 120° and larger, reaching a maximum as high as 2.8 at photon energies of 700-800 Mev. At higher photon energies, the ratio at backward pion angles also decreases with increasing photon energy.

The absolute cross-sections for positive pion photoproduction from deuterium have been determined and compared

to the corresponding cross-sections from hydrogen. This comparison should give some indication of the extent of the influence of the deuteron structure on the photoproduction process. The ratio of cross-sections for positive pion production from deuterium and hydrogen averages about 0.95. The scattering in the experimental results makes any attempts at interpretation suspect.

II. EQUIPMENT

The bremsstrahlung beam of the Caltech electron synchrotron passed through a liquid deuterium target. The total energy in the beam was measured by integrating the current from a Cornell type thick-walled ionization chamber which was placed in the beam after the target. The ionization chamber had been calibrated by R. Gomez (7). The liquid deuterium was contained in a thin-walled Mylar cup. Insulation from the outer atmosphere was provided by a vacuum chamber surrounding the cup. A reservoir filled with boiling hydrogen cooled the target cup and its contents below the boiling point of the deuterium.

Charged particles produced in the target were detected by the magnetic spectrometer system shown schematically in Figures 1a and 1b. The spectrometer was assembled in two different configurations. In Configuration I, the "high energy" configuration, the spectrometer was capable of focussing particles of momentum up to 1200 Mev/c. In Configuration II, the "medium energy" configuration, the spectrometer focussed particles of momentum up to only 600 Mev/c, while the solid angle for particle acceptance was larger. The field of the magnet was measured by a proton resonance magnetometer. The details of the design of the spectrometer and of the magnetometer unit are discussed in a separate report by P. L. Donoho (8).

A scintillation counter, S_A, placed near the entrance of the magnet aperture was used to help define the aperture and to reduce the background from particles which did not pass through the magnet. Since the counter was placed several inches

Figure 1a. MAGNETIC SPECTROMETER IN CONFIGURATION I

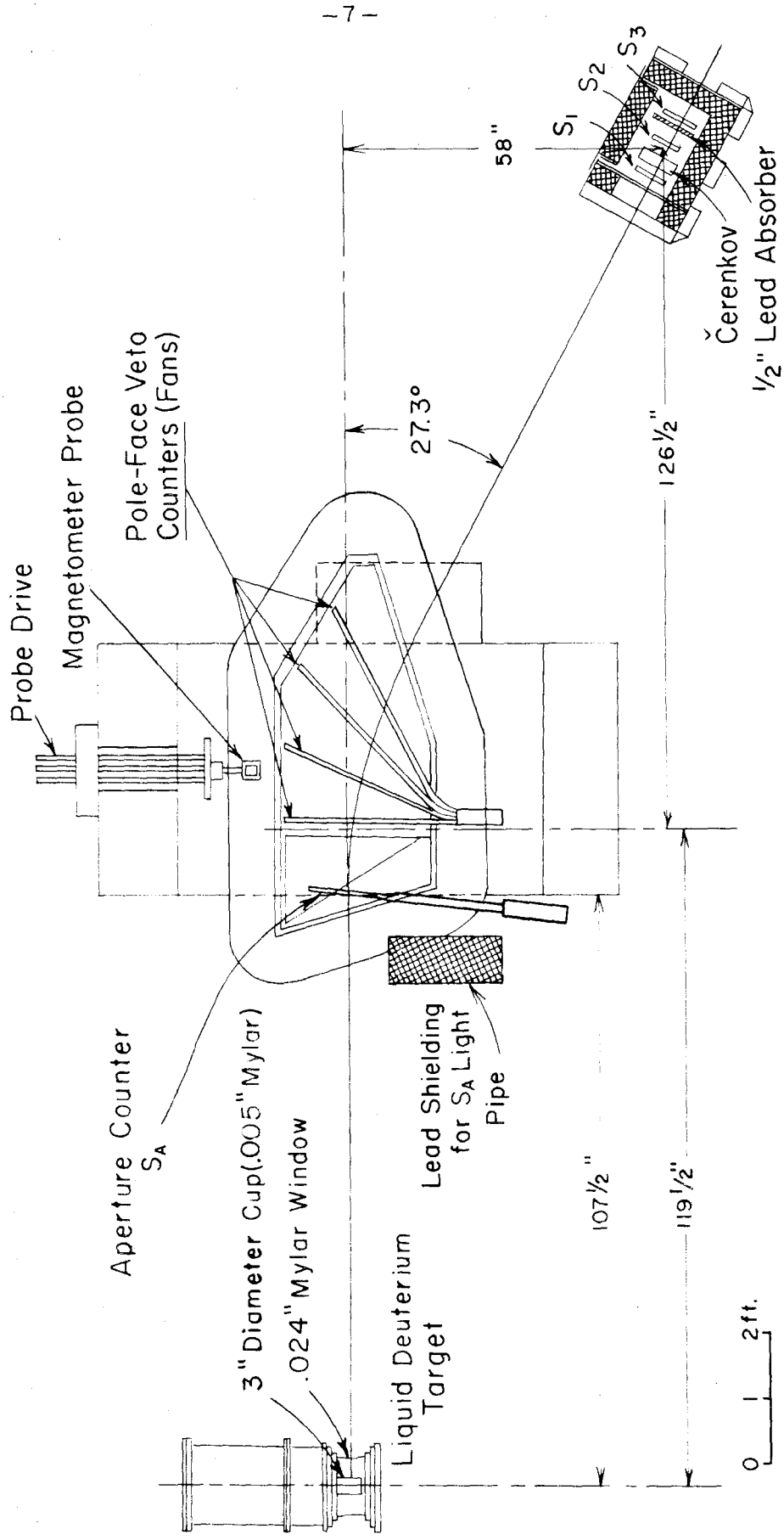
Probe Drive
Magnetometer Probe
Pole-Face Veto Counters (Fans)
27.3°
58"
126½"
S1
S2
S3
Čerenkov
½" Lead Absorber
Aperture Counter SA
3" Diameter Cup(.005" Mylar)
.024" Mylar Window
Liquid Deuterium Target
Lead Shielding for SA Light Pipe
107½"
119½"
0
1
2ft.

Figure 1b. MAGNETIC SPECTROMETER IN CONFIGURATION II

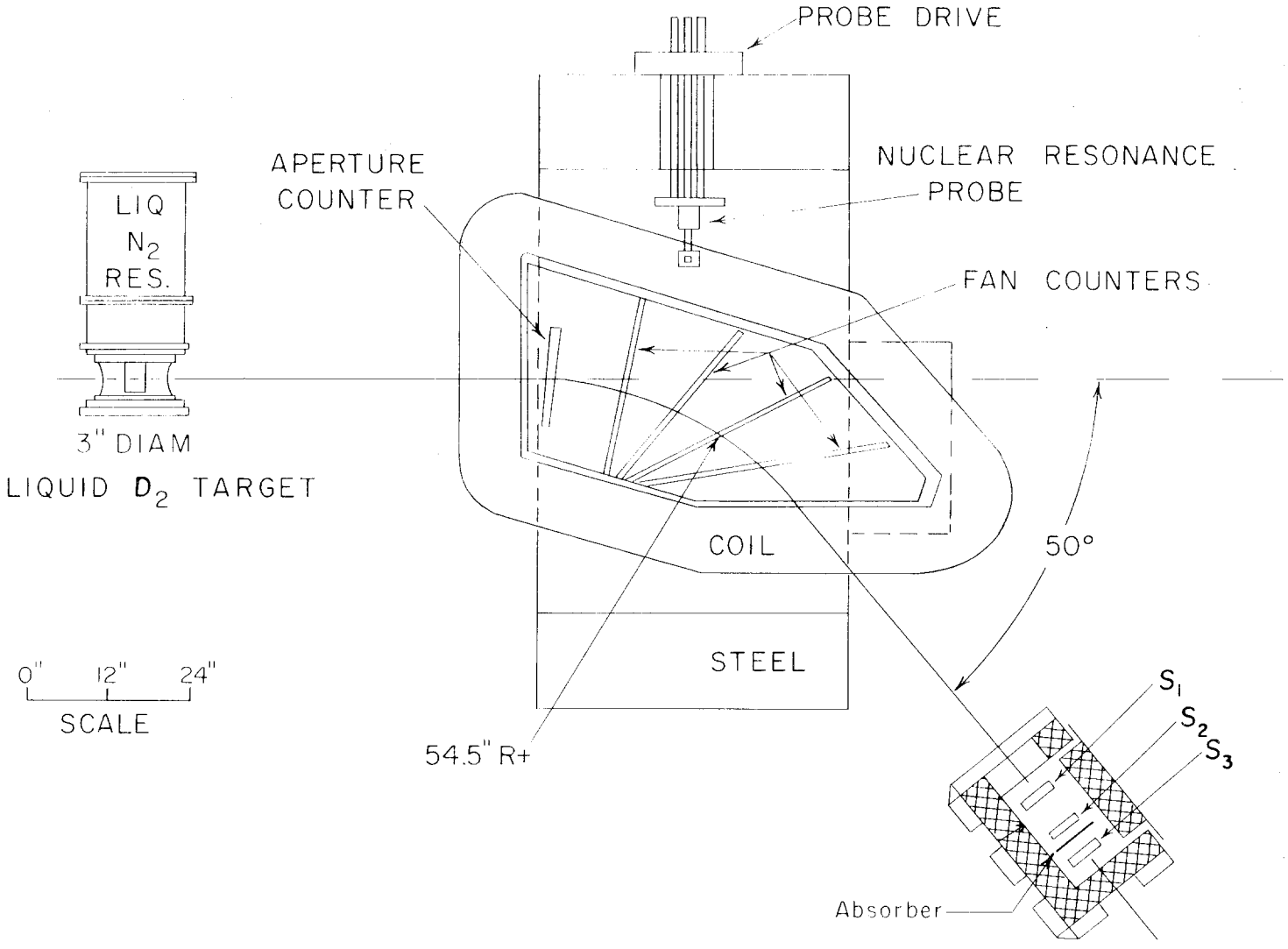
PROBE DRIVE
APERTURE COUNTER
NUCLEAR RESONANCE PROBE
FAN COUNTERS
LIQ N_2 RES.
3" DIAM
LIQUID D_2 TARGET
COIL
50°
STEEL
0" 12" 24"
SCALE
54.5" R+
S_1
S_2
S_3
Absorber

inside the edge of the magnetic field, the large flux of low energy charged particles produced in the target was deflected from the counter, and possible problems due to high counting rates in the counter were avoided.

Four narrow "fan counters" were placed along the surface of each of the magnet pole faces to help define the spectrometer aperture and to eliminate particles which might have scattered from the pole faces into the rear counters.

A set of three scintillation counters was used at the rear of the magnet to count those particles of the proper momentum which had passed through the magnet. S_2, the narrowest of the rear counters, defined the momentum interval accepted by the system. A lucite Cerenkov counter was added to the rear counter set during runs made with Configuration I of the spectrometer.

A few of the important parameters of the spectrometer system are listed below:

	Conf. I	Conf. II
Solid Angle ($\Delta\Omega$) of acceptance of spectrometer from target for particles of momentum P_o, where P_o is central momentum accepted by system (ster.)	.00197	.00603
Relative momentum acceptance ($\Delta P/P_o$)	.0992	.0989
Central distance from target to defining counter (inches)	260.5	165.0

Photomultipliers converted the light signals from the counters to electrical pulses, which then were identified by the

electronics system. An oscilloscope-camera system was used to monitor pulses from events identified as pions. A block diagram of the electronics appears as Figure 2.

Figure 2. ELECTRONICS BLOCK DIAGRAM

The resolving time of the fast coincidence circuits used was 30 mμs. The model 100 and the 6-channel coincidence circuits had resolving times of about 0.2μs. The rise time of the Model 522A amplifier was .07μs. The HP 460A was a distributed amplifier with a rise time of 2.7 mμs. The dashed lines shown in the diagram are circuits used only in Configuration I. In Configuration II the signals from S_2 were put into Channel 4 of the Discriminator. This channel was then run in anti-coincidence.

The numerals 6810 and 6655 refer to RCA Type 6810 and RCA Type 6655 photomultiplier tubes.

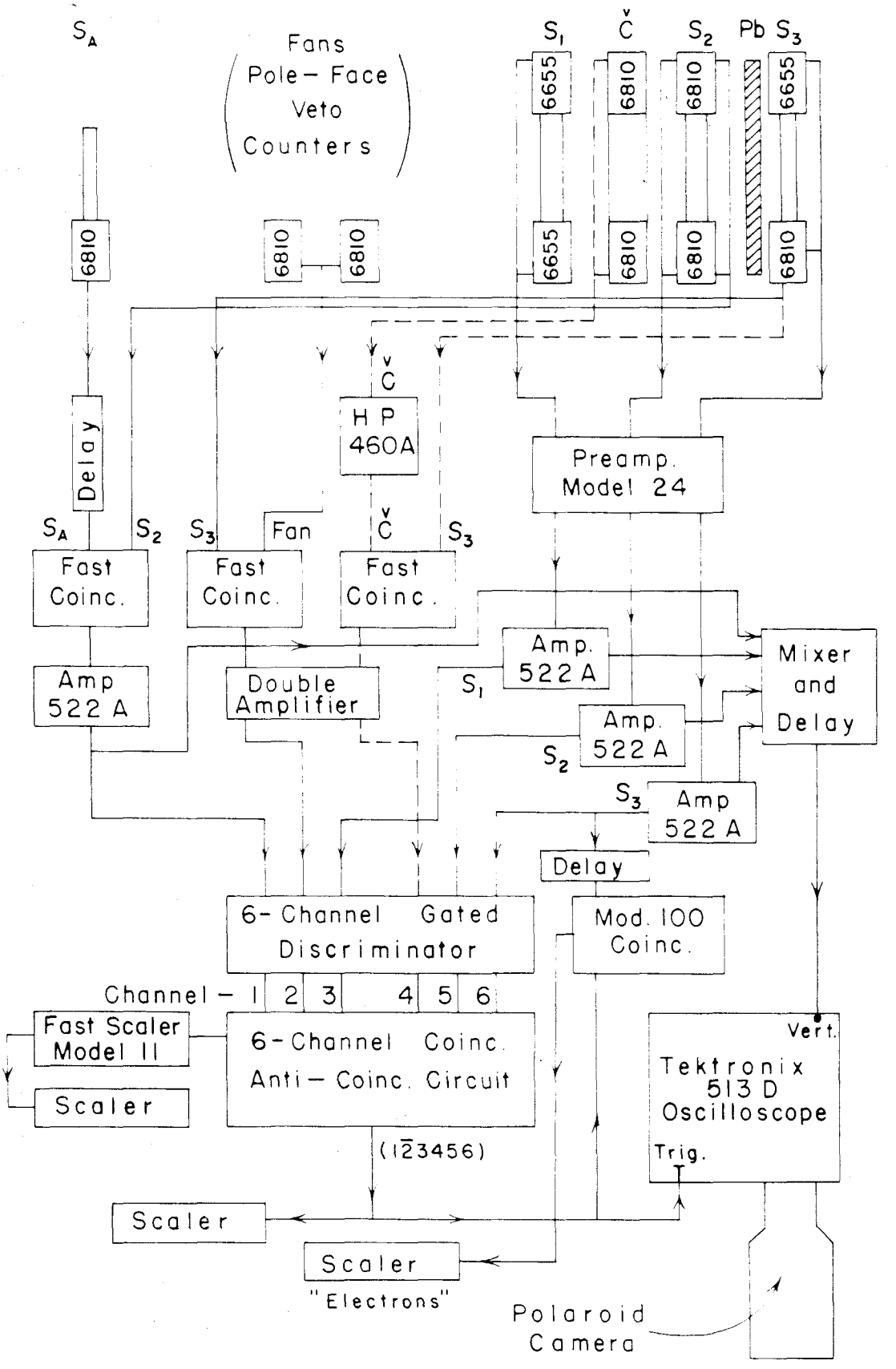

ELECTRONICS BLOCK DIAGRAM

III. EXPERIMENTAL PROCEDURE

The running of this experiment involved measuring the particle counting rates at various angular and momentum settings of the spectrometer. At each setting of the spectrometer the measurements were made in at least two runs on different days. During any one run the positive and negative pion counting rates were alternately measured. In this manner errors due to slow drifts in the equipment calibration were minimized.

Since the beam monitor was sensitive to variations of temperature and pressure, these factors were measured regularly, and the observed counting rates reduced to equivalent counting rates at 0°C, 760 mm.

A. Spectrometer Settings

The results of measurements from free nucleons are usually expressed as functions of the incident photon energy and of the pion center-of-mass angle. This experiment attempted to measure the photoproduction of charged pions from deuterium as a function of these same variables, so that a comparison with experiments from free nucleons might be readily made. Photon energies of 500, 600, 700, 800, 900, and 1000 Mev, and pion center-of-mass angles of 20°, 40°, 60°, 90°, 120°, and 150° were selected to give an overall picture of the entire energy interval considered. When it appeared that larger pion angles might provide interesting information, measurements were made at pion center-of-mass angles of 163°. This was the largest angle permitted by the physical limitations of the spectrometer and of the experimental area.

When the photon energy and pion center-of-mass angle have been selected in an experiment performed from free nucleons, the pion momentum and direction, in the laboratory, can be determined from the unique kinematic relationship which exists between the photon energy and the momentum and direction of the pion produced. This relationship is destroyed by the motion of the nucleons within the deuteron. A specific setting of the spectrometer momentum and angle corresponds to a range of photon energies and pion center-of-mass angles.

In this experiment, the spectrometer settings have been determined from the kinematic relationships which exist for photoproduction from free nucleons. It has been assumed that although these settings do not correspond to unique values of the photon energy and pion center-of-mass angle, the averages of these quantities will be the same as the values initially selected. A later calculation on the actual effects of the nucleon motion within the deuteron indicates that this assumption was justified.

The kinematic relationships which were used to determine the spectrometer settings are shown graphically in Figure 3. The actual values of the pion laboratory angle and momentum which were determined from these relationships are shown in Table 1.

The pions lose some energy between the target and the center of the spectrometer due to ionization losses in the air, the target, and the aperture counter. Because of these losses the actual settings of the spectrometer were, typically, 3 Mev/c below the values shown in Table 1.

Figure 3. KINEMATIC CURVES FOR PION PHOTOPRODUCTION FROM FREE NUCLEONS

k = photon energy (Mev)

P_π = pion momentum in laboratory (Mev/c)

θ_π = angle, in laboratory, between pion and photon beam (degrees)

θ^*_π = angle between pion and photon beam in center-of-mass system (degrees)

The solid curves represent constant photon energies. The dashed curves represent constant pion center-of-mass angles.

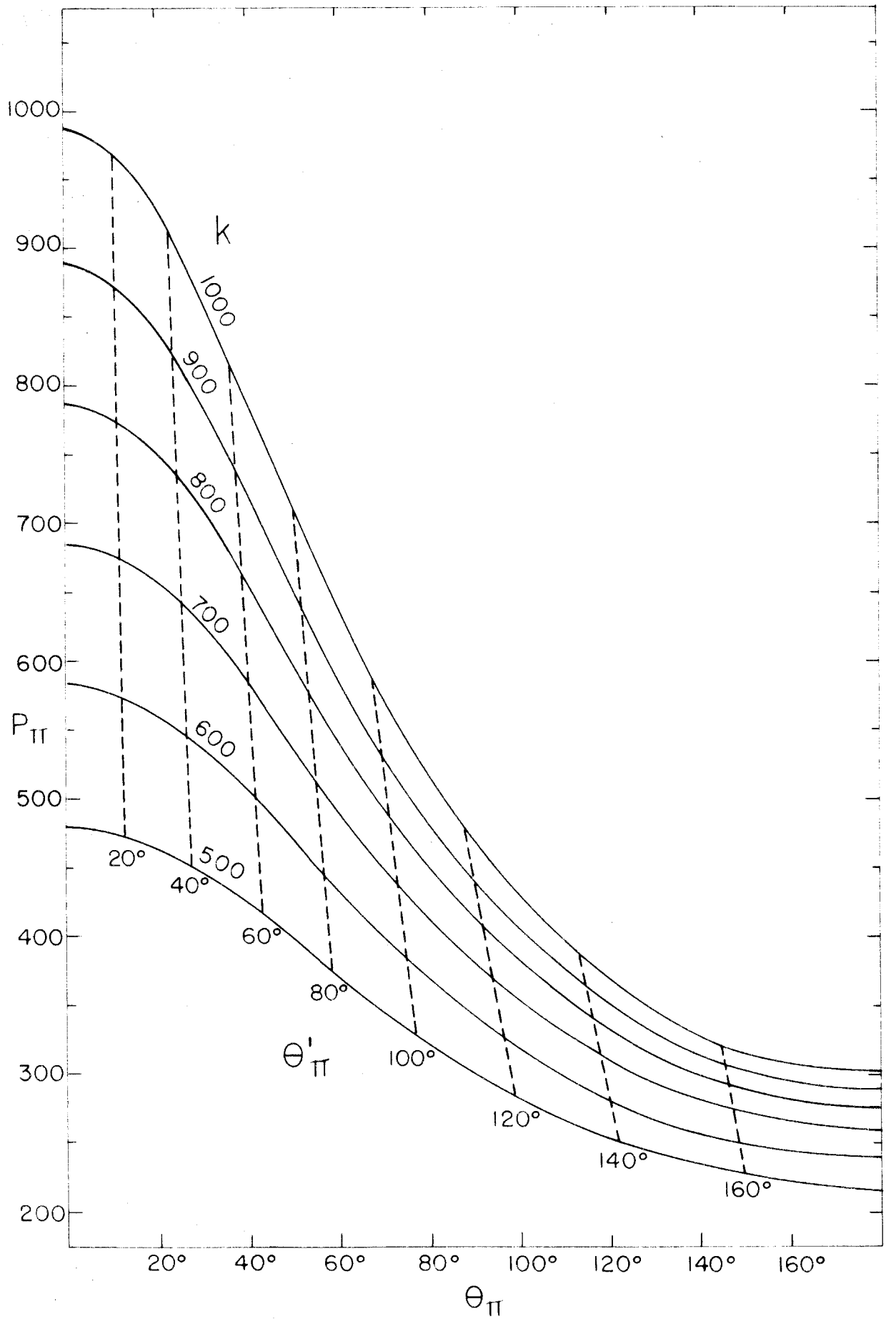
1000
900
800
700
600
500
400
300
200
P_{π}
k
1000
900
800
700
600
500
20°
40°
60°
80°
100°
120°
140°
160°
θ'_{π}
20°
40°
60°
80°
100°
120°
140°
160°
θ_{π}

Table 1. EXPERIMENTAL SETTINGS

k = nominal photon energy selected

θ_{CM} = pion center-of-mass angle selected

θ_{lab} = pion laboratory angle

= angle between spectrometer and photon beam

P_o = momentum at production of pions detected

E_o = endpoint energy of synchrotron at which measurements were made

k(Mev)	θ_{CM}(degrees)	θ_{lab}(degrees)	P_o(Mev/c)	E_o(Mev)
500	20	13.7	471	600
	40	27.8	450	
	60	42.8	417	
	90	68.0	352	
	120	98.5	287	
	150	136.1	236	
	161	151.5	225	
600	20	13.1	572	700
	40	26.7	545	
	60	41.1	501	
	90	65.7	417	
	120	96.0	333	
	150	134.5	265	
	162	151.5	250	
700	20	12.6	672	800
	40	25.6	636	
	60	39.5	582	
	90	63.6	478	
	120	93.7	373	
	150	132.6	291	
	162	151.5	271	
800	20	12.2	772	900
	40	24.6	728	
	60	38.1	663	
	90	61.6	537	
	120	91.5	410	
	150	130.9	313	
	163	151.5	289	
900	20	11.7	869	1000
	40	23.8	820	
	60	36.9	743	
	90	59.8	595	
	120	89.5	445	
	150	129.3	334	
	164	151.5	304	
1000	20	11.4	969	1080
	40	23.0	911	
	60	35.7	822	
	85	55.0	651	
	100	67.0	593	
	120	87.5	481	
	150	127.9	351	
	164	151.5	317	

B. Electron Identification

After the particles had passed through the magnet, it was necessary to differentiate pions from other charged particles which were also present. Since only electrons and protons, in addition to pions, were likely to be present in significant numbers, these were the only sources of contamination considered.

At the time the experiment was begun, it was assumed that there would be a significant number of electrons coming through the apparatus in at least some of the settings of the spectrometer. Therefore, appropriate measures were taken to eliminate these particles. A sheet of lead, one half of an inch thick, was placed between S_2 and S_3. Electrons would produce showers when passing through such a sheet, while pions, in general, would be unaffected. The shower fragments from the electron would produce a large pulse in S_3, which might then be used to identify the electron.

After the experiment was completed, some tests were made to determine the actual amount of electron contamination present. The yields of positive and negative events were measured from a hydrogen-filled target. Since protons, at the momentum considered, could not pass through the counting system, the measured yields were assumed to be composed of pions and electrons.

It is expected that the electron yield from hydrogen will be about evenly divided between positive and negative electrons. However, in the absence of a significant number of neutron targets, the pion yield should be composed almost entirely of positive pions.

Under these circumstances, the ratio of those events which gave large pulses in S_3 to those events which were nearly minimum ionizing should be enhanced for the negative field runs. No evidence for such an enhancement was found. The yields for negative particles from the hydrogen target were the same, within statistics, as the yields for negative particles from an empty target. Therefore, it was concluded that no electrons were passing through the spectrometer. Similar measurements, made earlier in conjunction with another experiment (4), indicated that no significant number of electrons was produced at the spectrometer settings used in this experiment. The use of the lead sheet was therefore probably unnecessary.

During the course of the experiment, it was observed that about 10 per cent of the counting rate was due to events which gave large pulses in the final counter. Inasmuch as it had been determined that no electrons were present, these events were attributed to pions which had interacted in the lead. Because large pulses in S_3 were useful in discrimination against protons, such events were always subtracted from the overall yields. It was assumed that the absorption correction for the lead, which was used to determine the absolute cross-sections, included a correction for the pions which were discarded in this manner.

C. Proton Identification

Although protons, at the momenta considered, had longer transit times through the apparatus than did pions, this factor was not used to separate the two types of particle. If the resolving time of the coincidence circuit used in conjunction with the

aperture counter had been shortened sufficiently to distinguish protons from pions, a certain amount of inefficiency would have been introduced into the circuit. Since this inefficiency could not be measured easily, no attempt was made to make such a transit time measurement.

At momenta below about 500 Mev/c, the separation problem is resolved quite simply, since protons of this momenta do not have sufficient energy to reach the final counter, and are not detected at all. At momenta up to about 700 Mev/c the protons, although they reach the final counter, are extremely heavily ionizing. The separation from the pions may then be made easily on the basis of the pulse heights in the counters. At higher momenta, as the protons become more nearly minimum ionizing, it becomes increasingly difficult to identify protons solely on the basis of their ionization losses. It was for this reason that the lucite Cerenkov counter was added to the counter system in Configuration I. Since this counter was sensitive only to particles with β greater than about 0.7, most of the protons, at momenta up to 1000 Mev/c, were not counted by it.

In Configuration I those events which either caused large pulses in S_3 or failed to trigger the fast coincidence circuit associated with the Cerenkov counter were discarded. In this manner most of the protons were eliminated. However, because the efficiency of the Cerenkov counter for detecting protons was not identically zero, it was necessary to correct the observed counting rates for a small proton contamination. The counting rate for protons which passed through the apparatus without

giving a large pulse in S_3 was measured by using the Cerenkov counter in anti-coincidence. This counting rate, when multiplied by the efficiency of the Cerenkov counter for counting protons, (see Section D below) gave the proton counting rate which was present in the corresponding pion runs. This counting rate was never more than 6 per cent of the observed pion counting rate.

In Configuration II both S_2 and S_3 were used to discriminate against the heavily ionizing protons. The proton contamination in the measured counting rates was less than 0.5 per cent, and has been neglected.

D. Efficiencies

At intervals during the course of the experiment, the efficiencies of the various components were measured. These measured efficiencies were then used to correct the measured yields.

The aperture counter, in coincidence with one of the rear counters, insured that the particles detected had actually come through the magnet. The resolving time of this coincidence circuit was set at about 30 mμs. This time was sufficiently short to eliminate any high accidental counting rate due to the relatively high flux of particles hitting the aperture counter. At the same time, this resolution time is long enough, relative to the spread in transit time of the pions through the apparatus, that its efficiency could be very high. Oscilloscope pictures of the output pulses from the coincidence circuit indicated that the efficiency of the circuit was probably greater than 98 per cent. Since no exact measurements were made on the efficiency of this circuit,

the possible small inefficiency was neglected.

The resolution time of the coincidence circuit associated with the aperture counter was reduced to about 4 mμs. to measure the efficiency of the Cerenkov counter. This short resolution time made it possible to separate pions from protons on the basis of their transit times through the apparatus. The "pure" beams of pions or protons which were defined by the transit time measurement were used to measure the efficiency of the Cerenkov counter for counting each type of particle. The results of these measurements are shown in Figure 4.

Since the efficiency of the Cerenkov counter for counting pions had no effect on the π^-/π^+ ratio, the measurement of this efficiency was not made very carefully. Unfortunately, the pion efficiency does affect the values of the differential cross-sections for positive pion photoproduction. A more complete discussion of the pion efficiency of the Cerenkov counter will be found in Section VI. A-3, where the effect of counter inefficiencies on the determination of the absolute values of the positive pion cross-sections is considered.

Since the photomultipliers are very sensitive to magnetic fields, a measurement was made to determine whether a large shift in the magnetic field strength would appreciably change the phototube gains, and thus the counting efficiencies. The results of such a measurement, for one counter, are shown in Figure 5. Measurements made on other counters of the rear counter set showed similar effects. Although the photomultipliers associated with the fan counters and with the aperture counter were in regions

Figure 4. CERENKOV EFFICIENCIES

ε_P = efficiency for counting protons

ε_π = efficiency for counting pions

P = particle momentum (Mev/c)

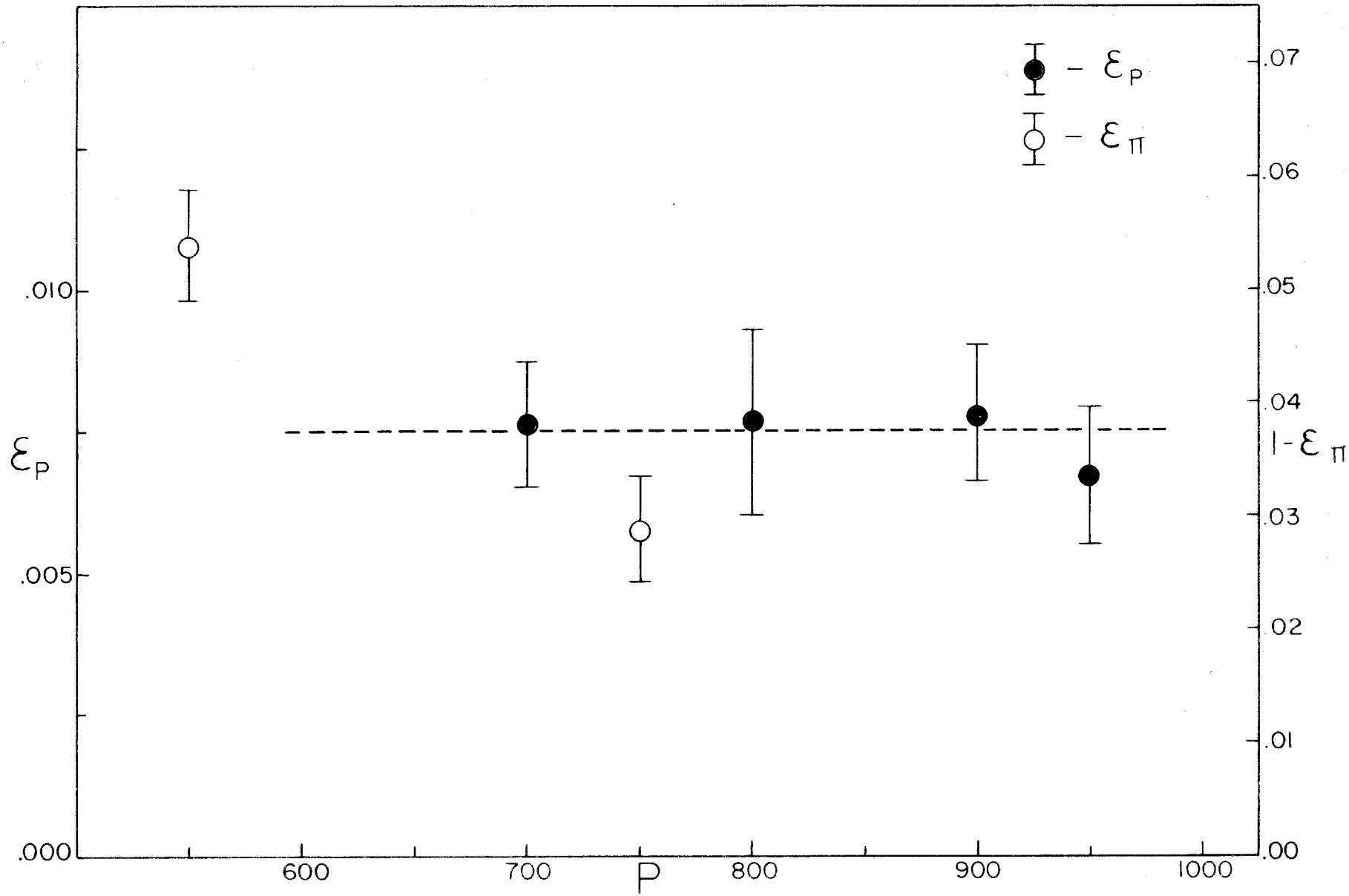
● - ε_p
○ - ε_π
.010
.005
.000
ε_p
.07
.06
.05
.04
.03
.02
.01
.00
$1-\varepsilon_\pi$
600
700
800
900
1000
P

Figure 5. PULSE HEIGHT DISTRIBUTION

The figure shows the pulse height distribution for pions in S_2. Two runs were made with opposite values of the magnetic field (plus and minus 15,000 gauss). The actual channel numbers of the pulse height analyzer are shown across the top of the figure, while the corresponding voltage is shown at the bottom. Field changes between 0 and 15,000 gauss also appeared to have little effect on the phototube gain.

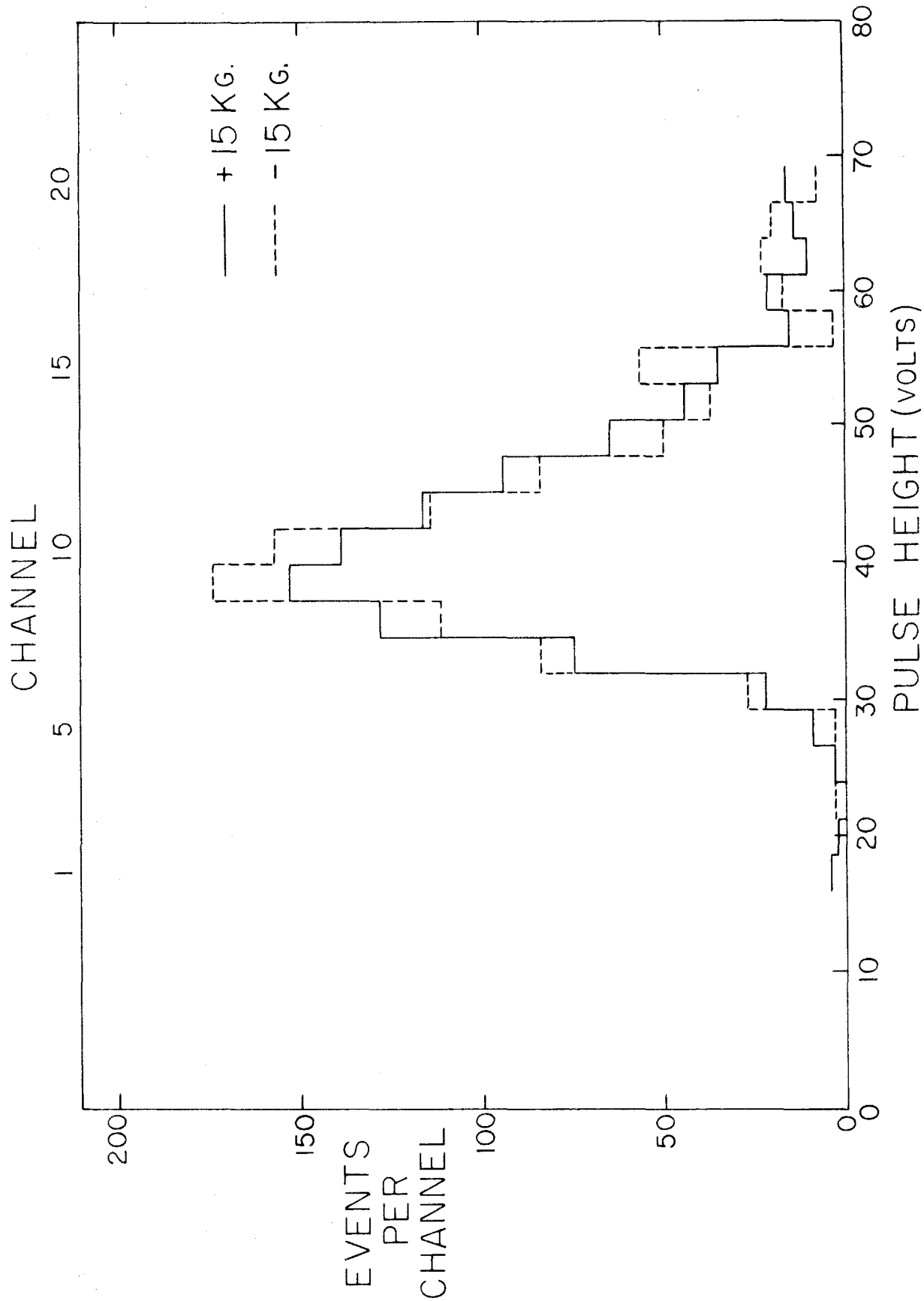
CHANNEL
1
5
10
15
20
+ 15 KG.
- 15 KG.
EVENTS PER CHANNEL
200
150
100
50
0
10
20
30
40
50
60
70
80
PULSE HEIGHT (VOLTS)

of relatively high magnetic field strength, they were shielded in such a manner that changes in the field strength did not change their gains by more than 20 per cent (9). Changes of this magnitude in the pulses from the counters would not affect the operation of the fast coincidence circuits to which they were sent.

The lower biases of the discriminators were set at 15 volts for S_1, S_2, and S_3. As may be seen from Figure 5, this bias is well below the bottom of the pion pulse height distributions. The loss in counting rate due to pion pulses falling below this bias could not have been as large as 0.5 per cent. This possible inefficiency has been neglected.

E. Backgrounds

The background counting rates from the target material were measured with the deuterium removed from the target cup. These counting rates were typically about 10 per cent of the rates measured with the target full. Due to an oversight, no proton counting rates were measured from the target material. The background proton counting rates which appear in Table 3 have been taken from a previous experiment which used the same target (4).

F. Target Contamination

During the course of the experiment, the deuterium used was analyzed* several times. These analyses showed that the deuterium became increasingly contaminated with hydrogen and several heavier elements. Certain opaque substances coated

*The analyses were made with a mass spectrometer by Consolidated Electrodynamics Corporation, Pasadena, California

the wall of the target cup when deuterium was put into the target. This coating, which was assumed to be the heavier contamination, settled to the bottom of the target cup, out of the path of the photon beam, within a few hours. Therefore the contamination by the heavier elements was neglected.

The temperature of the target contents during the runs was that of hydrogen boiling under a pressure of $2\frac{1}{2}$ pounds above atmospheric. ("Atmospheric" averaged about 740 mm during the experiment.) The density of pure hydrogen at this temperature (20.7°K) is .0700 gm/cc, while that of pure deuterium is .1693 gm/cc (10).

The effective density of the hydrogen in the target may be written as:

$$(\rho_H)_{eff.} = \rho_H \frac{V_H}{V_H + V_D}$$

where V_H = volume occupied by hydrogen

V_D = volume occupied by deuterium

ρ_H = pure hydrogen density = .0700 gm/cc

The effective density of the hydrogen may be written as:

$$(\rho_H)_{eff.} = \rho_H \frac{a/\rho_H}{a/\rho_H + (1-a)/\rho_D}$$

$$= \frac{\rho_D a}{1 + \frac{a(\rho_D - \rho_H)}{\rho_H}}$$

$$= \frac{.1693\ a}{1 + 1.42a}$$

where:

ρ_D = density of pure deuterium = .1693 gm/cc

a = fraction of total number of nucleons which are hydrogen

$$a = \frac{\text{no. of hydrogen atoms}}{2 \times \text{deuterium atoms} + \text{hydrogen atoms}}$$

A similar expression can be written for the effective deuterium density:

$$(\rho_D)_{eff.} = \frac{.1693\ (1-a)}{1 + 1.42\ a}$$

The results of the deuterium analyses and the density determinations are shown in Table 2. The counting rate due to the hydrogen was determined from the effective hydrogen density and the known cross-sections for the production of positive pions from hydrogen (4). This counting rate was subtracted from the observed counting rate of positive pions to find the rates due to the deuterium alone.

G. Pair Contamination

All of the runs, except those made at photon energies of 1000 Mev, were made with the bremsstrahlung endpoint of the synchrotron beam 100 Mev above the nominal photon energy used. This endpoint would have always been low enough to avoid counts from multiply-produced pions from free nucleons. In this experiment, however, the motion of the nucleons within the deuteron makes energetically possible some contamination from multiply-produced pions. Measurements of the π^-/π^+ ratio as a function of the bremsstrahlung endpoint were made at several selections of the pion momentum (11). These measurements indicated that multiple pion production caused no change in the observed ratio, within statistical limits, for bremsstrahlung endpoints several hundred Mev above the endpoints actually used.

Table 2. TARGET ANALYSIS

$$a = \frac{\text{no. of hydrogen atoms}}{2 \times \text{no. of deuterium atoms} + \text{no. of hydrogen atoms}}$$

	Configuration I			Configuration II		
Date of sampling	Oct. 25	Nov. 11	Dec. 18	Dec. 26	Feb. 12	Mar. 18
Mol % D_2	98.67	97.89	96.67		93.93	94.12
Mol % H_2	.70	.67	.95		1.33	1.10
Mol % HD	.55	1.44	1.48		3.06	3.81
Mol % O_2 + N_2, etc.	.08	.00	.90		1.68	.97
α	.0049	.0070	.0086		.0148	.0154
Effective Deuterium Density (gm/cc)	.1673	.1665	.1658		.1634	.1630
Effective Hydrogen Density (gm/cc)	.0008	.0012	.0015		.0025	.0027

No sampling made at the beginning of runs in Configuration II

Density Values used in Calculations

The errors in the values of the effective deuterium density, due to possible errors in the evaluation of the density of pure deuterium, are $\pm$ .0005 gm/cc. The errors in the values of the effective hydrogen density, due to possible errors in the evaluation of the densities of pure deuterium and pure hydrogen, are less than $\pm$ .0001 gm/cc.

IV. CROSS-SECTION FORMULA

The counting rate, in counts per BIP, for the photoproduction of pions from nucleons, is given by:

$$C = \int_k \int_z \int_x \int_y \int_{\Delta\Omega} \frac{d\sigma}{d\Omega'} \frac{d\Omega'}{d\Omega} \, d\Omega \; n(k) \; f(x, y) \; \eta \; R \; A \; \varepsilon \; dxdydzdk$$

where:

$\frac{d\sigma}{d\Omega'}$ is the differential cross-section in the center-of-mass (CM) system

$\frac{d\Omega'}{d\Omega}$ is the ratio of differential solid angle in the center-of-mass system to that in the laboratory

η is the density of nucleons in the target

$n(k)$ is the number of photons per Mev-BIP in the beam, as a function of k, the photon energy

A is the fraction of pions which are not absorbed before they can be counted

R is the decay correction factor (See appendix)

ε is the overall efficiency of the apparatus for counting pions

$f(x, y)$ represents the lateral beam distribution at the target, normalized so that $\int f(x, y)dxdy = 1$

x, y, z are coordinates of position in the target, relative to the center of the target.

A BIP (Beam Integrator Pulse) is a standard amount of charge collected from the ion chamber which monitors the photon beam

The xy plane is taken perpendicular to the direction of the photon beam.

This formula must be simplified before any practical use may be made of it. Since the target is far from the magnet aperture, and since the pions lose very little energy in the target, the integration over the target variables may be performed independently of the other variables:

$$\int f(x, y)\, \eta\, dxdydz = \frac{\rho N_o \bar{l}}{M}$$

where:

M is the atomic weight of the target material

ρ is the density, in gm/cm^3, of the target material

N_o is Avogadro's number (6.0235×10^{23})

$\bar{l}$ is the effective length of the target along the direction of the photon beam.

The number of photons in the beam, n(k), is given by:

$$n(k) = \frac{W\, B(k, E_o)}{E_o\, k}$$

where:

E_o is the endpoint energy of the bremsstrahlung spectrum

W is the total energy per BIP in the beam

$\frac{B(k, E_o)}{k}$ is the relative number of photons of each energy in the beam

The counting rate now reduces to:

$$C = \frac{\rho N_o \Gamma W A R \epsilon}{M\ E_o} \int \frac{d\sigma}{d\Omega'} \frac{d\Omega'}{d\Omega}\, d\Omega \frac{B(k, E_o)dk}{k}$$

If the variations of $d\sigma/d\Omega'$ and $d\Omega'/d\Omega$ over the angles accepted by the magnet aperture are neglected, the integral over the magnet solid angle may be performed. If the differential cross-section is assumed to vary linearly over the limits of the

variation of the photon energy, the cross-section may be replaced by an average value of the cross-section, and taken outside of the integral:

$$\int \frac{d\sigma}{d\Omega'} \frac{d\Omega'}{d\Omega} \, d\Omega \frac{B(k, E_o)}{k} \, dk = \overline{\frac{d\sigma}{d\Omega'}} \int \frac{d\Omega'}{d\Omega} \frac{B(k, E_o)}{k} \, \Delta\Omega \, (P) \, dk$$

where:

$\overline{\frac{d\sigma}{d\Omega'}}$ is the value of the differential cross-section measured at

$$\bar{k} = \frac{\int \frac{d\Omega'}{d\Omega} \Delta\Omega(P) \; B(k, E_o) \; dk}{\int \frac{d\Omega'}{d\Omega} \Delta\Omega(P) \; \frac{B(k, E_o)}{k} \; dk}$$

$\Delta\Omega(P)$ is the solid angle of the spectrometer as a function of the pion momentum P

At this point, an expression for the differential cross-section may be extracted:

$$\overline{\frac{d\sigma}{d\Omega'}} = C \left[\frac{\rho N_o \bar{l} \, W \, R \, A \, \epsilon}{M \, E_o} \int \frac{d\Omega'}{d\Omega} \Delta\Omega(P) \frac{B(k, E_o)}{k} \, dk \right]^{-1}$$

The integral which remains in the expression above is the response of the apparatus.

The apparatus response which is defined above is readily evaluated for experiments done from free nucleons. In an experiment performed from deuterium, however, the relationship between the pion momentum P and the photon energy k will depend on the internal momentum of the target nucleons. A more careful analysis of the apparatus response must be made before the cross-section formula derived above can be applied to an experiment

from deuterium.

The momentum distribution of the nucleons within the deuteron was assumed to be close to that given by the Hulthen wave function. For any given target nucleon momentum, the relationship between k, P, and K, the incident photon energy in the rest system of the target nucleon, may be found. The response of the apparatus for any value of K was determined by averaging:

$$\frac{d\Omega'}{d\Omega}\ \Delta\Omega\,(P)\ \frac{B(k, E_o)}{k}\ \frac{dk}{dK}$$

over the momentum distribution of the nucleons. The integral over K of this averaged quantity,

$$\int \overline{\frac{d\Omega'}{d\Omega}\ \Delta\Omega\,(P)\ \frac{B(k, E_o)}{k}\ \frac{dk}{dK}}\ dK = \int \mathcal{R}\,(K)\ dK,$$

is the response of the apparatus for photoproduction from deuterium. The effective photon energy at which the measurements are made is the average value of K over this response function:

$$\overline{K} = \frac{\int K\,\mathcal{R}(K)dK}{\int \mathcal{R}(K)dK}$$

A detailed discussion of the calculations which have been made for the nucleon motion has been given by Mr. G. Neugebauer (11).

A typical plot of $\mathcal{R}\,(K)$ appears as Figure 6. The curve which would have been obtained in the absence of nucleon motion is shown for comparison. As the figure indicates, the nucleon motion results in spreading the response over a larger range of photon energies.

The nucleon motion calculations indicated that the average pion center-of-mass angle was within 2 per cent of the nominal center-of-mass angle selected.

Figure 6. NUCLEON MOTION EFFECT ON APPARATUS RESPONSE

The solid curve shows the apparatus response as a function of K, assuming no motion of the target nucleons. The dashed curve shows the response, under the same conditions, when the motion of the nucleons is considered.

The response, $\mathcal{R}(K)$, is plotted in units of 10^{-5} ster/Mev as a function of the photon energy in the rest system of the target nucleon. The curves drawn are for the spectrometer settings corresponding to nominal photon energy and pion center-of-mass angle of 700 Mev, 20^{o}. For larger angles, both response curves extend over wider photon energies. A more detailed description of these effects has been given by Mr. G. Neugebauer (11).

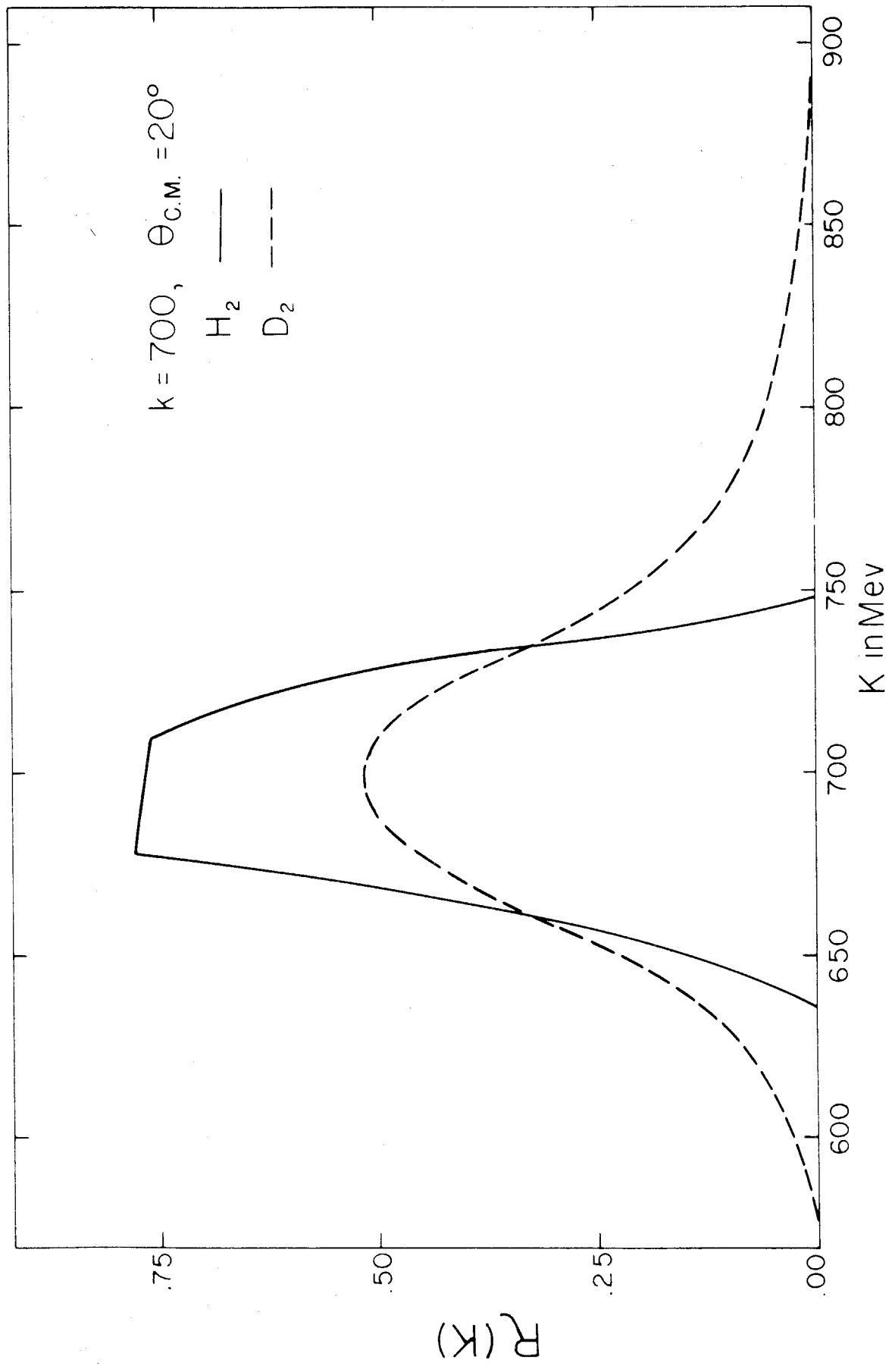
k = 700, θc.m. = 20°
H2
D2
R(K)
.00
.25
.50
.75
600
650
700
750
800
850
900
K in Mev

V. RATIO OF NEGATIVE TO POSITIVE CROSS-SECTIONS

A. Calculations

The ratio of differential cross-sections for charged pion photoproduction from deuterium will be given by:

$$\frac{\frac{d\sigma^-}{d\Omega'}}{\frac{d\sigma^+}{d\Omega'}} = \frac{C^- \left[\frac{W\rho N_o T R^- A^- \varepsilon^-}{E_o \quad M} \int \mathcal{R}(K)dK \right]^{-1}}{C^+ \left[\frac{W\rho N_o 1 R^+ A^+ \varepsilon^+}{E_o \quad M} \int \mathcal{R}(K)dK \right]^{-1}}$$

Cancelling those factors which are identical, we have:

$$\frac{\frac{d\sigma^-}{d\Omega'}}{\frac{d\sigma^+}{d\Omega'}} = \frac{\pi^-}{\pi^+} = \frac{C^- R^+ A^+ \varepsilon^+}{C^+ R^- A^- \varepsilon^-} = \frac{C^-}{C^+} A^* R^* \varepsilon^*$$

where A^*, R^*, and ε^* are the ratios of the correction factors. Since no difference in the counter efficiencies was noted for counting positive and negative pions, ε^* may be set equal to unity. The discussion of the decay effects (see appendix) indicates that R^* may also be set equal to unity.

About 20 per cent of the total number of pions were absorbed between production and detection, mostly by the lead and by the counter material. Measurements made on the absorption in the lead (11) indicated that no difference existed for positive and negative pions. It is known, however, that a difference exists in the scattering cross-sections of negative and positive pions from hydrogen. Since the counters contain hydrogen, the absorption in them should be different for positive and negative pions. The values of A^* which result from this difference have been calculated (11).

Although this correction makes less than a 2 per cent change in the π^-/π^+ ratios, it has been included in the calculations.

B. Results

The results of the measurements on the proton contamination are shown in Table 3. The final results of the π^-/π^+ ratio determinations are shown in Table 4. The ratios are plotted at each pion center-of-mass angle as functions of the effective photon energy in Figures 7-13.

C. Errors

The errors which are listed with the ratios in Table 4 are the composite statistical errors in the counting rates. Small (less than 1 per cent) errors due to uncertainties in the effective hydrogen density, in the absorption calculations, and in the proton contamination have been neglected.

The values of $\overline{K}$, the effective photon energies at which the π^-/π^+ ratio is assumed to have been measured, have been calculated using a model for the deuteron which may not represent the actual situation. However, the values of $\overline{K}$ which have been obtained, except those at very backward pion angles, are not more than a few per cent different from the average photon energy which would have been computed in the absence of nucleon motion. It seems unlikely, therefore, that these values would be changed a great deal if some other model of the deuteron were used.

D. Discussion

Although this experiment has measured the ratio of the values of the differential cross-sections for negative and positive pion photoproduction from deuterium, the measurements were

Table 3. PROTON CONTAMINATION

k = nominal photon energy in Mev

θ_{CM} = pion center-of-mass angle in degrees

C_P = proton counting rates in counts/BIP

$C^{*'}_P$ = proton contribution to pion runs = $C_P \times \epsilon_p$

C^*_{PB} = proton contribution to background runs

$P = C^*_P - C^*_{PB}$ = proton contamination in pion counting rates from deuterium

k	θ_{CM}	C_P	C^*_P	C^*_{PB}	P
500	20	0.069	.001	----	.001
600	20	0.261	.002	----	.002
700	20	0.223	.002	----	.002
	40	0.139	.001	----	.001
	60	0.132	.001	----	.001
800	20	3.192	.024	.005	.019
	40	0.402	.003	.001	.002
	60	0.026	----	----	----
900	20	4.862	.036	.006	.030
	40	2.958	.022	.003	.019
	60	0.400	.003	.001	.002
1000	20	6.160	.046	.005	.041
	40	3.277	.024	.004	.020
	60	1.164	.009	.001	.008

Table 4. π^-/π^+ RATIOS

k = nominal photon energy, in Mev

θ_{CM} = nominal center-of-mass pion angle, in degrees

$\overline{K}$ = effective incident photon energy in Mev

N^+ = counting rate for positive particles from the entire target, in counts/BIP

B^+ = counting rate from empty target

P = counting rate from proton contamination

C_H = counting rate from hydrogen in target

C^+ = positive pion counting rate from deuterium

$= N^+ - B^+ - P - C_H$

C^- = negative pion counting rate from deuterium

A^* = absorption factor

The Roman numbers to the left of the pion center-of-mass angles indicate with which configuration of the spectrometer the data were taken.

k		θ_{CM}	$\bar{K}$	N^+	B^+	P	C_H	C^+	N^-
500	I	20	507	1.406	.134	.001	.026	1.246±.046	1.519
	II	40	507	4.315	.173	----	.153	3.989±.135	4.069
		60	508	3.520	.135	----	.106	3.279±.110	3.089
		90	506	1.719	.014	----	.050	1.655±.066	1.823
		120	505	.690	.032	----	.024	.634±.033	1.167
		150	498	.490	.047	----	.016	.427±.027	.918
		161	498	.514	.116	----	.013	.385±.035	.973
600	I	20	605	1.519	.149	.002	.026	1.342±.149	1.758
	II	40	608	4.865	.408	----	.157	4.300±.160	4.125
		60	609	3.899	.180	----	.125	3.594±.138	3.030
		90	607	1.717	.061	----	.061	1.595±.062	1.705
		120	599	.692	.015	----	.028	.649±.032	1.009
		150	590	.378	.035	----	.015	.328±.023	.842
		162	588	.392	.072	----	.012	.308±.128	.867

k		θ_{CM}	B^-	C^-	C^-/C^+	A*	π^-/π^+
500	I	20	.125	1.394±.048	1.119	.995	1.113±.055
	II	40	.147	3.922±.132	.983	.995	.978±.046
		60	.153	2.936±.104	.895	.992	.888±.042
		90	.034	1.789±.068	1.081	.986	1.066±.059
		120	.042	1.125±.049	1.774	.982	1.743±.116
		150	.031	.887±.041	2.077	.989	2.054±.163
		161	.113	.860±.055	2.234	.990	2.211±.240
600	I	20	.113	1.645±.051	1.226	1.000	1.226±.061
	II	40	.332	3.793±.137	.882	1.000	.882±.046
		60	.204	2.826±.103	.786	.998	.785±.041
		90	.048	1.657±.062	1.039	.993	1.032±.054
		120	.028	.981±.042	1.512	.984	1.487±.094
		150	.065	.777±.042	2.369	.985	2.333±.198
		162	.095	.772±.049	2.506	.987	2.474±.266

k		θ_{CM}	$\bar{K}$	N^+	B^+	P	C_H	C^+	N^-
700	I	20	704	1.512	.134	.002	.026	1.350±.048	1.567
		40	704	1.494	.113	.001	.022	1.358±.049	1.222
		60	706	1.118	.078	.001	.018	1.021±.040	.869
	II	60	708	4.049	.181	----	.134	3.734±.115	3.074
		90	704	2.077	.055	----	.083	1.939±.049	1.605
		120	699	.846	.041	----	.032	.773±.025	.952
		150	682	.374	.045	----	.014	.315±.026	.813
		162	677	.349	.047	----	.011	.291±.028	.754
800	I	20	806	1.171	.153	.019	.020	.979±.040	.931
		40	804	1.028	.130	.002	.015	.881±.040	.774
		60	805	.795	.080	----	.010	.705±.031	.489
	II	90	801	1.317	.036	----	.044	1.237±.039	.896
		120	791	.676	.033	----	.023	.620±.025	.601
		150	769	.328	.017	----	.012	.299±.021	.570
		163	766	.229	.032	----	.009	.188±.018	.610

k		θ_{CM}	B^-	C^-	C^-/C^+	A*	π^-/π^+
700	I	20	.116	1.451±.049	1.075	1.006	1.081±.053
		40	.106	1.116±.040	.822	1.004	.825±.040
		60	.076	.793±.039	.777	1.001	.778±.050
	II	60	.112	2.962±.106	.793	1.001	.794±.037
		90	.058	1.547±.056	.798	.997	.795±.034
		120	.013	.939±.028	1.215	.989	1.201±.051
		150	.036	.777±.043	2.467	.982	2.422±.232
		162	.048	.706±.043	2.426	.984	2.387±.266
800	I	20	.083	.848±.035	.866	1.009	.874±.051
		40	.054	.720±.028	.817	1.008	.824±.051
		60	.032	.457±.021	.648	1.005	.651±.041
	II	90	.044	.852±.030	.689	.999	.688±.032
		120	.022	.579±.023	.934	.992	.926±.052
		150	.021	.549±.029	1.836	.982	1.803±.154
		163	.062	.548±.039	2.915	.982	2.862±.330

k		θ_{CM}	$\bar{K}$	N^+	B^+	P	C_H	C^+	N^-
900	I	20	903	1.181	.126	.030	.018	1.007±.035	.702
		40	904	1.087	.118	.019	.016	.934±.045	.572
		60	903	.627	.059	.002	.009	.557±.024	.299
	II	90	899	.792	.043	----	.025	.724±.033	.420
		120	882	.531	.011	----	.018	.502±.027	.316
		150	861	.269	.008	----	.010	.251±.018	.396
		164	851	.242	.046	----	.009	.187±.018	.447
1000	I	20	1003	.939	.125	.041	.015	.758±.035	.604
		40	1002	1.050	.069	.020	.021	.940±.042	.636
		60	1002	.650	.064	.008	.013	.564±.026	.281
		85	952	.233	.020	----	.003	.210±.015	.095
	II	100	988	.514	.036	----	.020	.455±.027	.302
		120	972	.457	.019	----	.020	.418±.027	.231
		150	937	.272	.021	----	.012	.240±.018	.322
		164	928	.230	.038	----	.009	.183±.015	.342

k		θ_{CM}	B^-	C^-	C^-/C^+	A*	π^-/π^+
900	I	20	.087	.615±.025	.611	1.007	.615±.034
		40	.060	.512±.023	.548	1.008	.553±.035
		60	.028	.271±.016	.487	1.008	.490±.035
	II	90	.017	.403±.020	.556	1.001	.557±.037
		120	.009	.307±.019	.612	.995	.609±.049
		150	.011	.385±.023	1.534	.984	1.509±.138
		164	.034	.413±.029	2.209	.981	2.167±.249
1000	I	20	.058	.546±.023	.720	1.007	.725±.043
		40	.036	.600±.028	.638	1.007	.643±.041
		60	.015	.266±.015	.472	1.009	.476±.033
		85	.011	.084±.006	.400	1.004	.402±.040
	II	100	.002	.300±.015	.659	1.001	.660±.050
		120	.020	.211±.017	.505	.997	.503±.050
		150	.012	.310±.020	1.292	.986	1.274±.122
		164	.020	.322±.018	1.760	.982	1.728±.164

Figures 7-13. π^-/π^+ RATIOS

In the following figures the final, corrected, values of the π^-/π^+ ratios are plotted as a function of $\overline{K}$, in Mev, for each center-of-mass pion angle at which measurements were made.

The solid circles represent measurements made previously in this laboratory by Sands, Teasdale, Walker, and Bloch (6). The open circles are the results of the present experiment.

The measurements at 700 Mev, 60° were made in each of the spectrometer configurations. The proximity of the two circles for these measurements indicates that the two configurations of the spectrometer gave consistent results.

At the bottom of several of the figures, for nominal photon energies of 500, 700, and 900 Mev, a small curve, which indicates the width of the apparatus response, has been plotted.

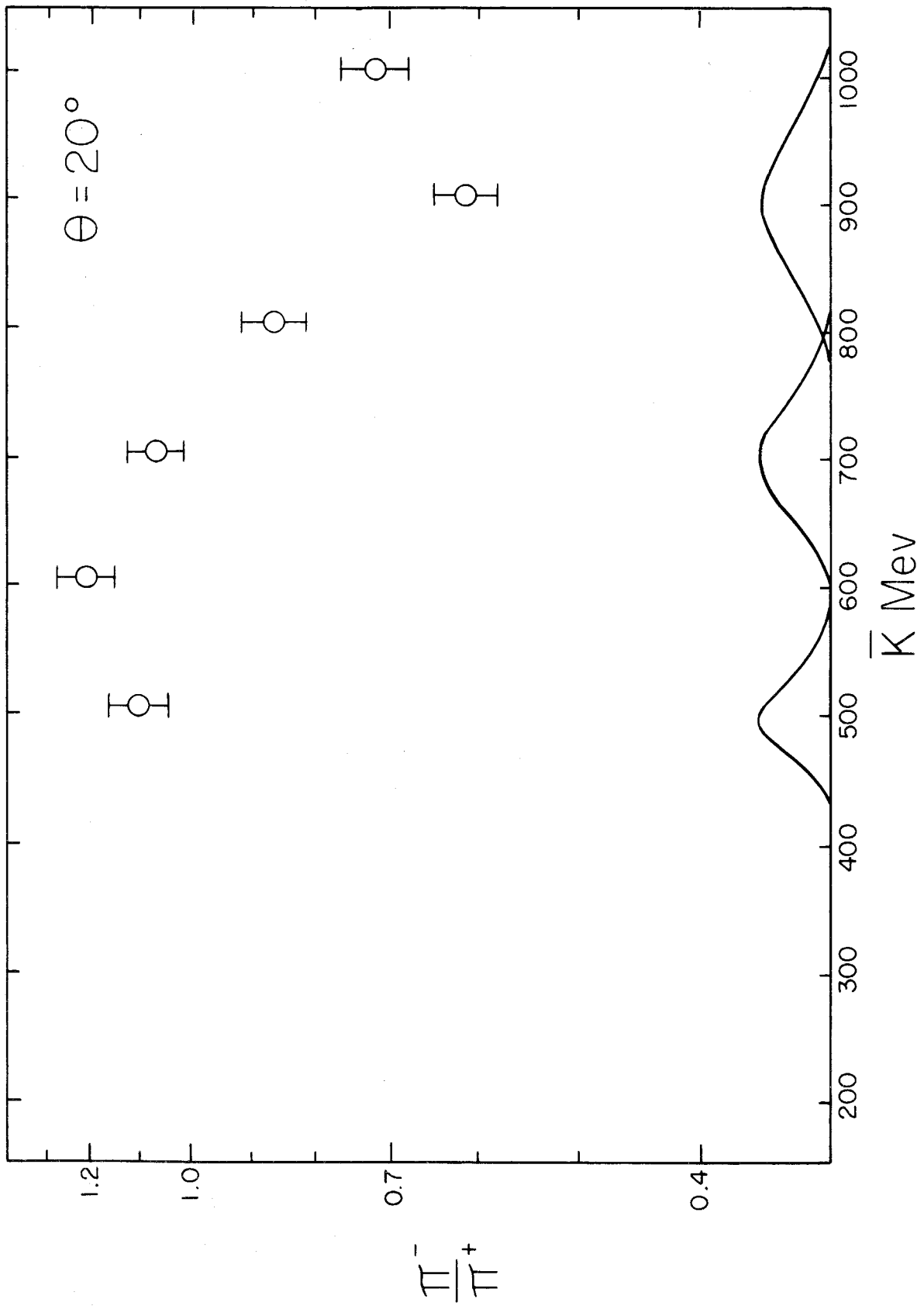
θ = 20°
π⁻/π⁺
1.2
1.0
0.7
0.4
200
300
400
500
600
700
800
900
1000
K̄ Mev

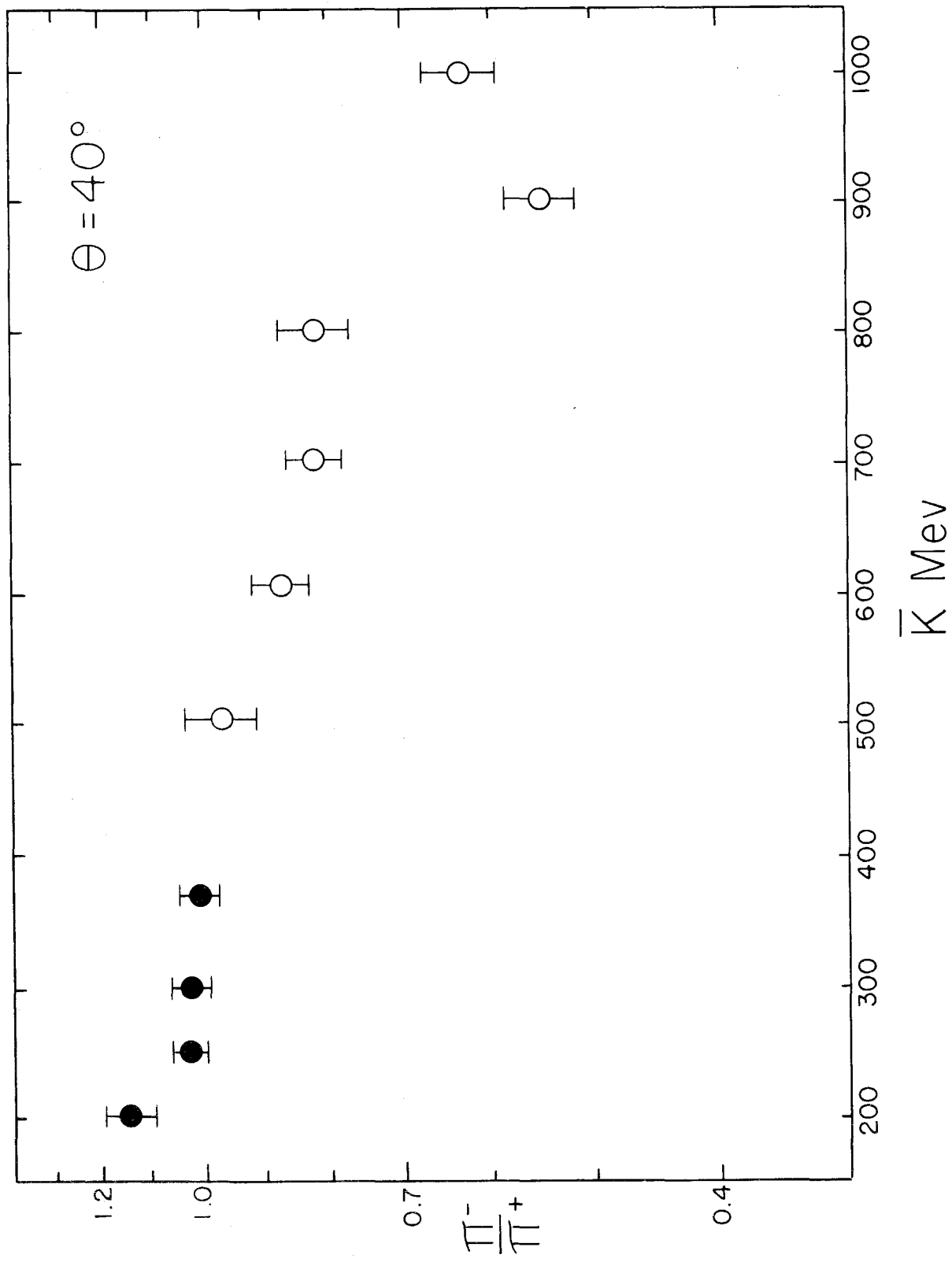
θ=40°
1.2
1.0
0.7
0.4
π⁻/π⁺
200
300
400
500
600
700
800
900
1000
K̄ Mev

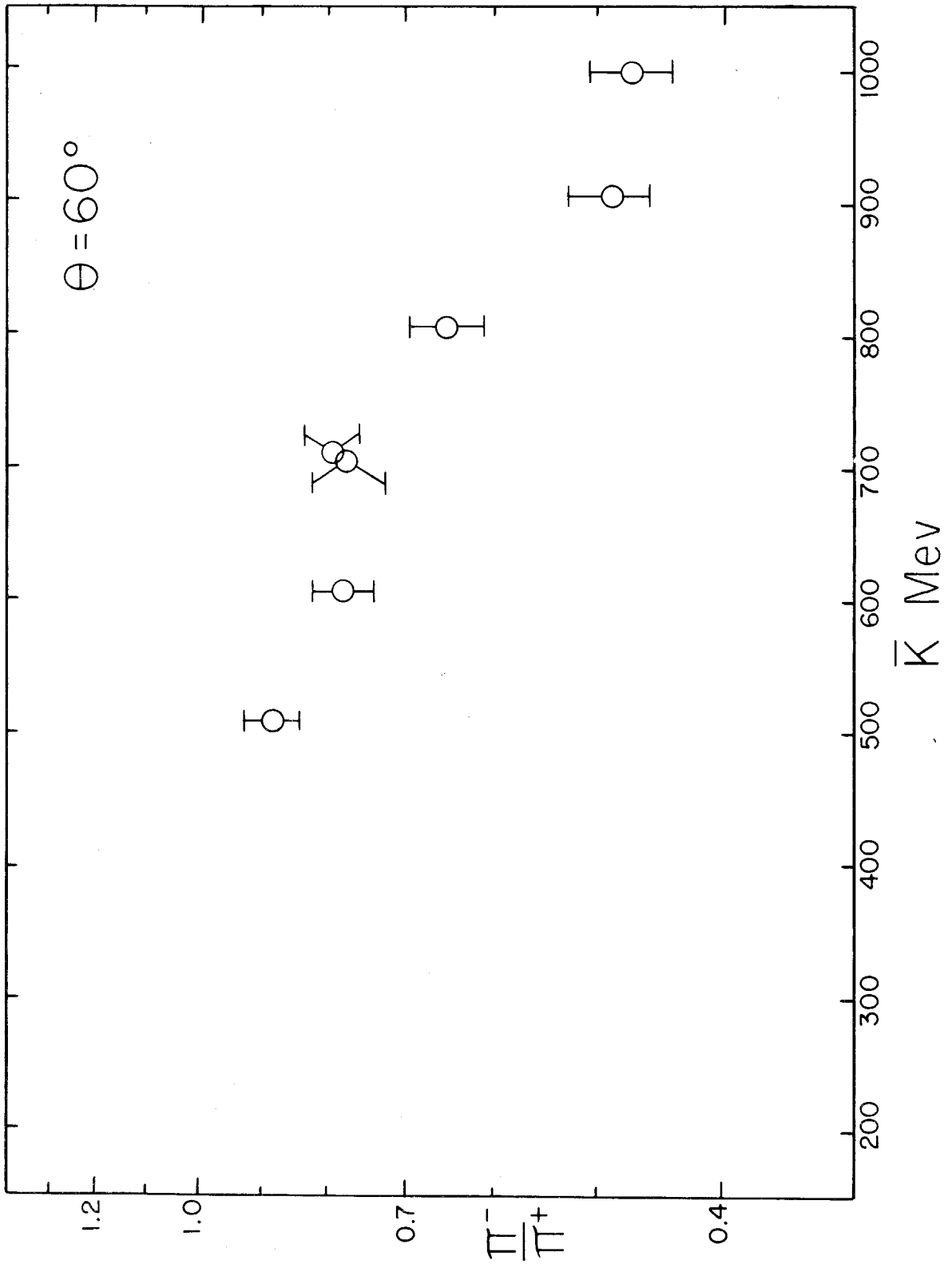
θ=60°
1.2
1.0
0.7
0.4
π⁻/π⁺
200
300
400
500
600
700
800
900
1000
K̄ Mev

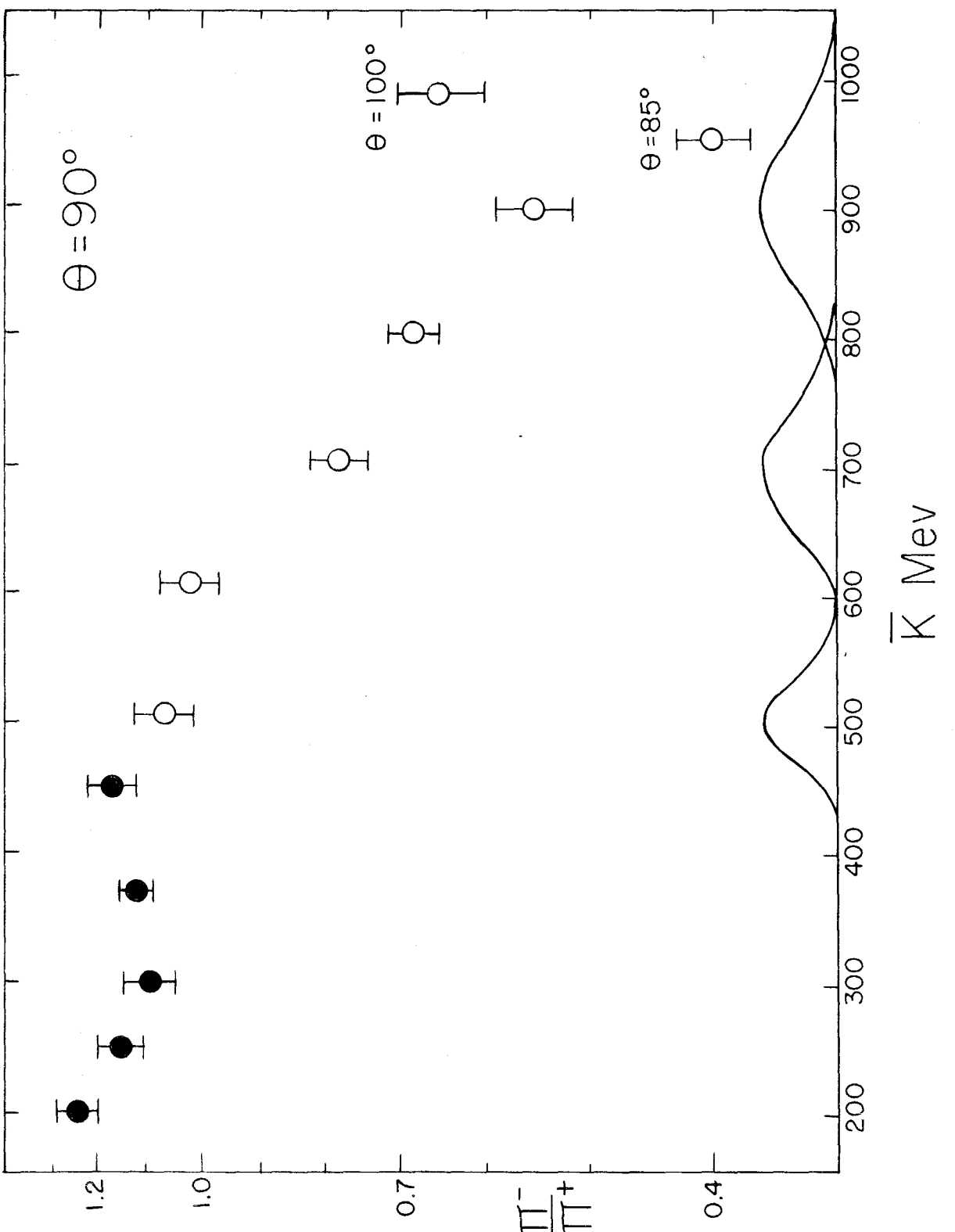
θ=90°
θ=100°
θ=85°
1.2
1.0
0.7
0.4
π⁻/π⁺
200
300
400
500
600
700
800
900
1000
K̄ Mev

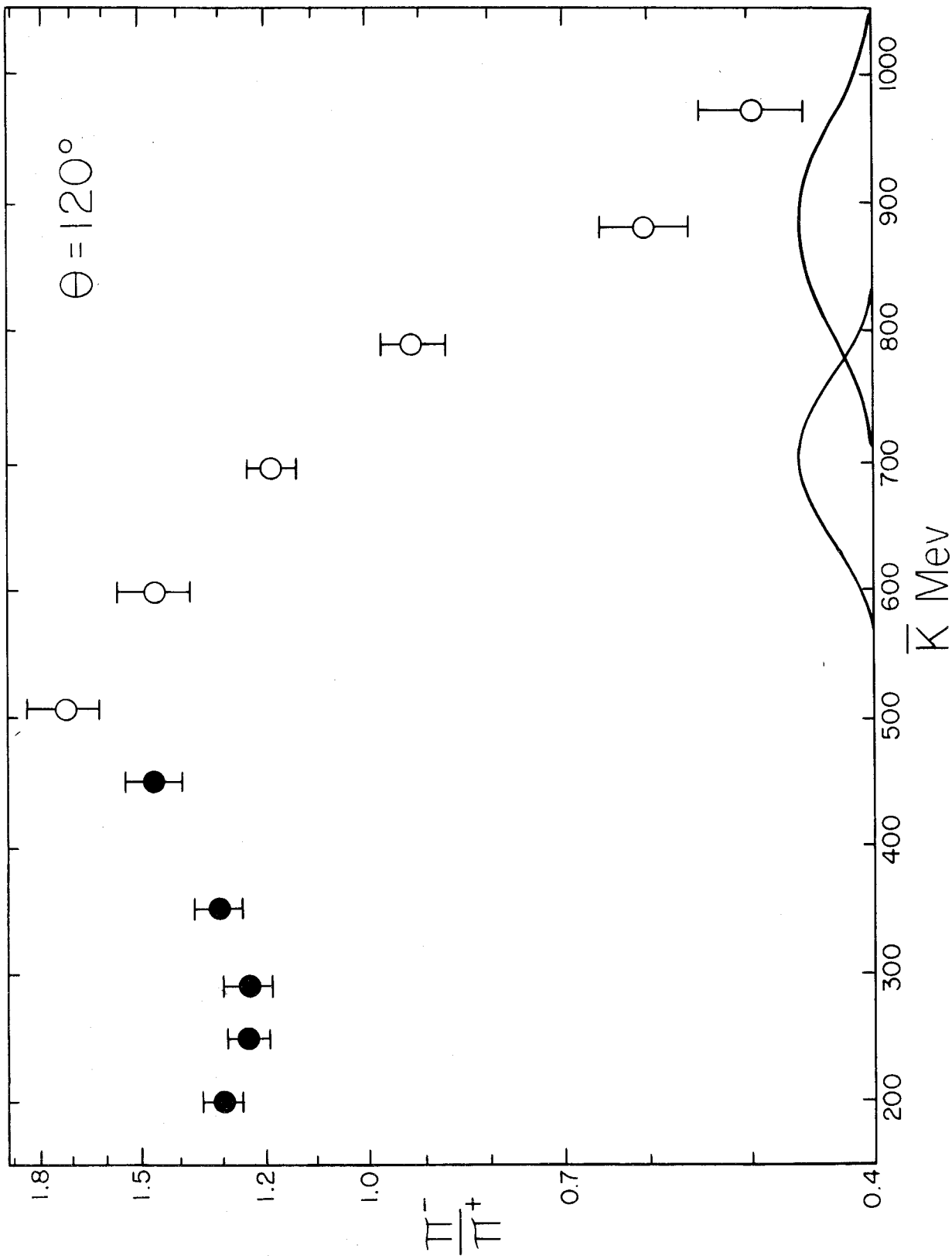
θ=120°
π⁻/π⁺
1.8
1.5
1.2
1.0
0.7
0.4
200
300
400
500
600
700
800
900
1000
K̄ Mev

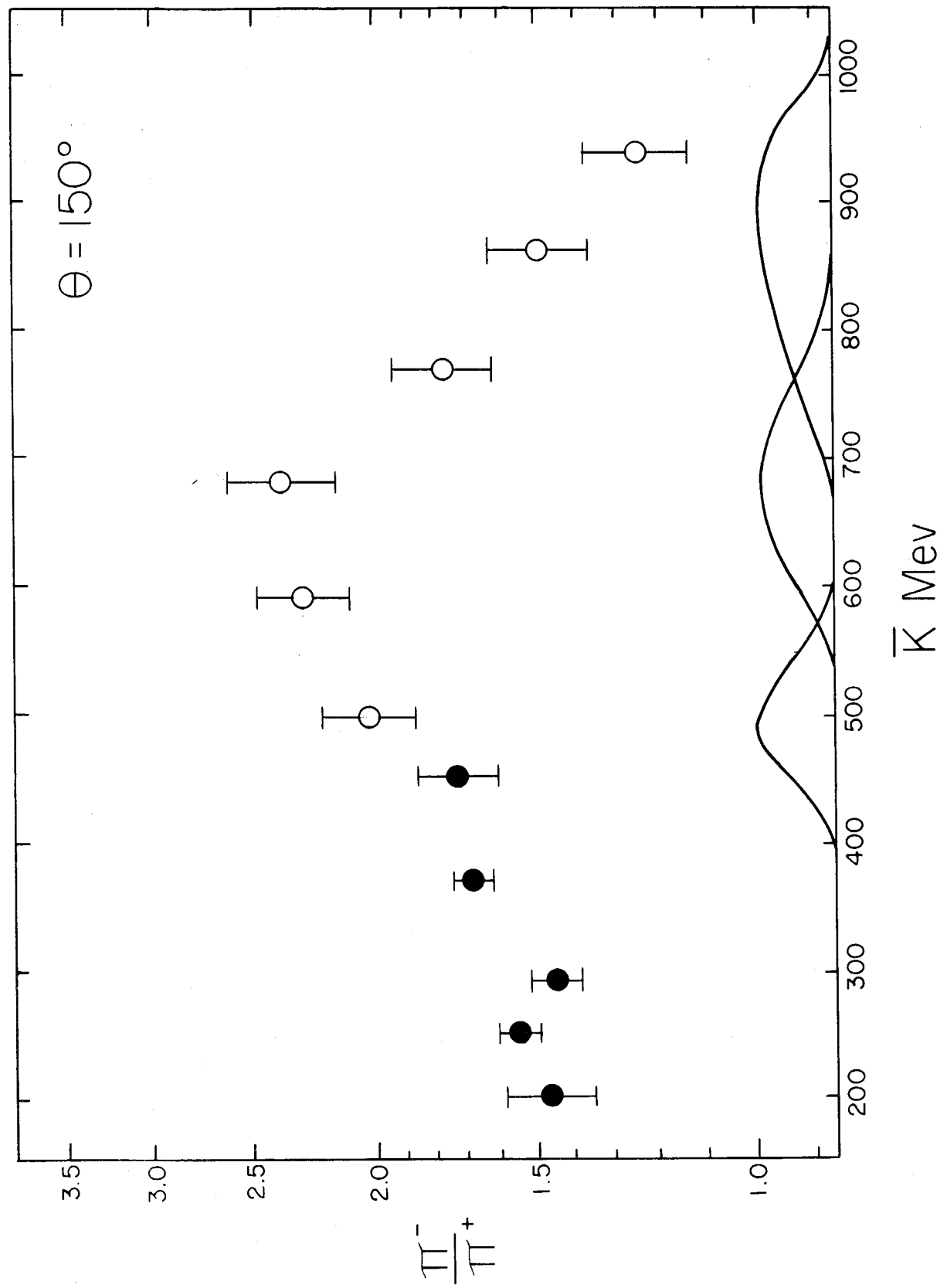
θ = 150°
$\frac{\pi^-}{\pi^+}$
3.5
3.0
2.5
2.0
1.5
1.0
200
300
400
500
600
700
800
900
1000
$\overline{K}$ Mev

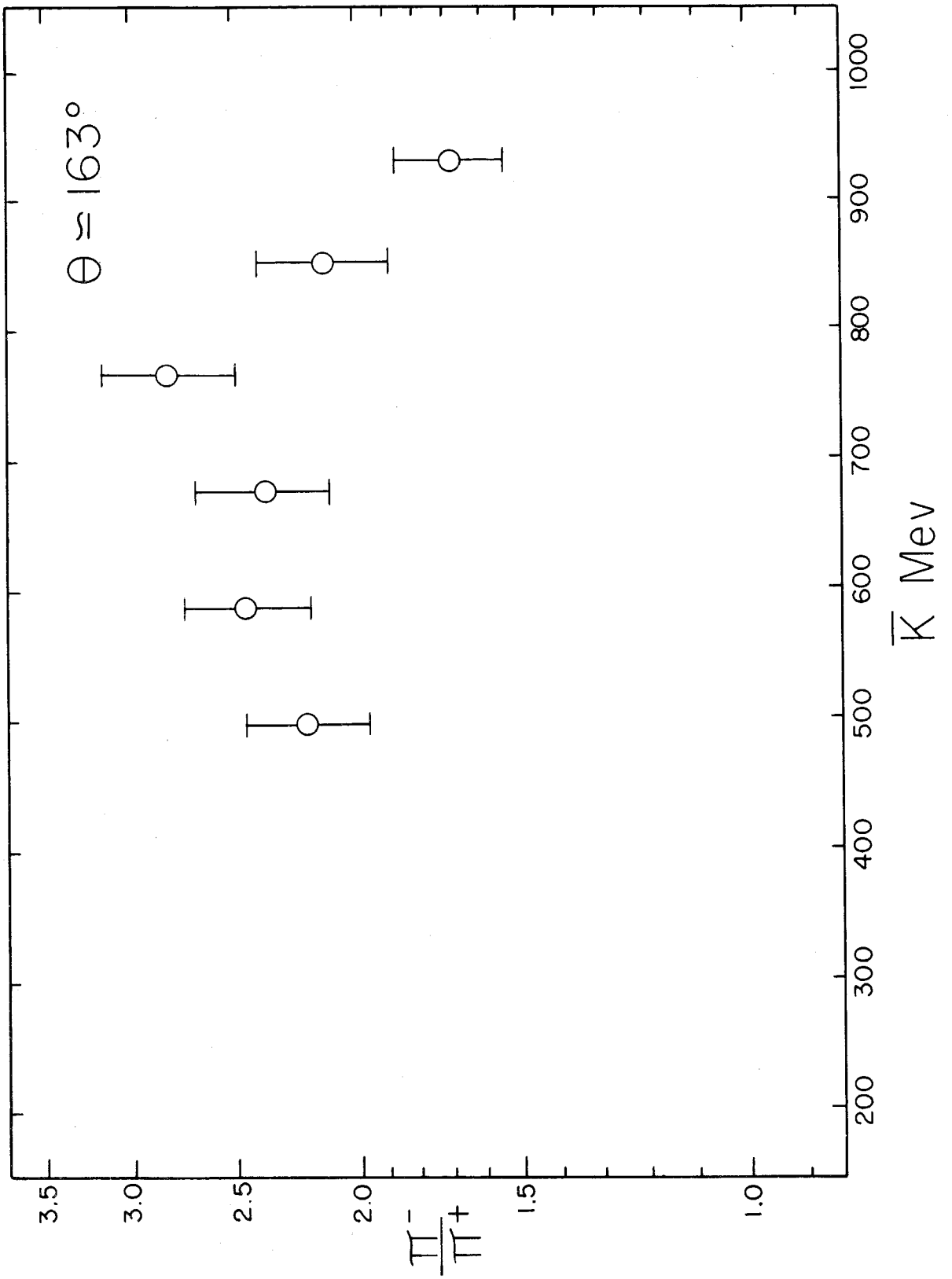
θ ≅ 163°
π⁻/π⁺
3.5
3.0
2.5
2.0
1.5
1.0
200
300
400
500
600
700
800
900
1000
K̄ Mev

made in the hope of getting information on the ratio of cross-sections from free nucleons. The relation between the π^-/π^+ ratio measured from deuterium and the corresponding ratio which would be measured from free nucleons may be seen by considering the factors which lead to a difference between the cross-sections measured from deuterium and from free nucleons.

At low energies, the difference in the coulomb effects on the reactions:

$$\gamma + n \longrightarrow \pi^- + p$$
$$\gamma + d \longrightarrow \pi^- + p + p$$

makes a small difference in the cross-sections. However, at the energies considered in this experiment, this effect should be entirely negligible.

The Pauli exclusion principle predicts that the cross-sections from deuterium should be reduced relative to those from free nucleons if the two nucleons from the deuteron are left adjacent and in the same spin state. However, this effect should be identical for both signs of pion. The effect of the exclusion principle in this experiment should be extremely small because of the high recoil energies involved.

When a photon excites one of the nucleons of a deuteron, it is possible that the entire deuteron will become excited. If this happens, the energy will be lost by the disintegration of the deuteron, either with or without the emission of one or more pions. Since this process competes with single pion photoproduction from the nucleons of the deuteron, the cross-sections

for single pion photoproduction will be reduced. This effect, however, should be quite small, since the probability that the entire deuteron will become excited if one of the nucleons is excited is less than 10 per cent. In addition, it seems likely that this effect, which depends on the overlapping of the nucleon wave functions, would affect positive and negative pion production in the same degree.

Since none of these factors have very much influence on the π^-/π^+ ratio, it may be concluded that the ratio from free nucleons would, if it could be measured, be the same as the ratios measured in this experiment.

From the data presented in Figures 7-13, several facts are evident. First, the agreement between this experiment and the previous experiment done on the π^-/π^+ ratio at this laboratory is very good at those places where a comparison can be made. Second, it appears that the general trend of the ratio with energy is down. This is in distinct contrast to lower energy data. The ratio increases with pion angle at all energies measured, as it did in lower energy measurements. There is a very slight indication that some change in the trend of the π^-/π^+ ratio with energy may be taking place at 1000 Mev, since several of the measurements at small angles indicate a higher ratio at 1000 Mev than at 900 Mev. However, this reversal of the trend with energy is not consistent enough to permit any conclusions.

The variation of the π^-/π^+ ratio at high energies near $\theta_{CM} \approx 90^\circ$ is somewhat puzzling. The equipment response in this region is spread over such a range of photon energies that such

a rapid variation with energy would be extremely difficult to measure. If it is assumed that the expected value of the ratio in this region is constant, at 0.52, which is near the average of the measurements, then the measurement made at $\overline{K} = 988$ Mev, $\theta_{CM} = 100^{o}$ is three standard deviations from the expected value, while the measurement made at $\overline{K} = 952$ Mev, $\theta_{CM} = 85^{o}$ is four deviations from the expected value. It is, therefore, not likely that statistical fluctuations might be the cause of this anomaly. It seems more reasonable to assume that one of the measurements is definitely wrong due to experimental difficulties, such as faulty counter gates or poor beam dump, which were not noticed at the time the measurements were made.

Except for this one region, the data appear to be self-consistent. The ratio, at 900 Mev, appears to be close to one-half for most pion angles.

As Watson has pointed out (12), the matrix elements for the photoproduction of charged pions in any one angular momentum state may be written:

$$T^{+} = \sqrt{2}\, T^{(3)} + 1/\sqrt{2}\left[T^{(1)} - \delta T^{(1)} \right]$$

$$T^{-} = \sqrt{2}\, T^{(3)} + 1/\sqrt{2}\left[T^{(1)} + \delta T^{(1)} \right]$$

where $T^{(3)}$ is the matrix element for the isotopic spin 3/2 state, and $T^{(1)}$ and $\delta T^{(1)}$ are the matrix elements corresponding to isotopic spin 1/2. For states with isotopic spin 3/2, the ratio of charged pions photoproduced from deuterium should be unity. For states of isotopic spin 1/2, the ratio will depend on the relationship between the two matrix elements for isotopic spin 1/2. Thus, in

theory, for production in a state with isotopic spin 1/2, the measured values of the π^-/π^+ ratio may be used to determine the relationship between the two matrix elements. In practice, because of the mixture of various isotopic spin and angular momentum states which exists at the points which can be measured, this determination, especially at high energies, is very difficult.

The data at lower energies have been given a fair qualitative fit by the simple classical explanations due to Bruckner (13). In this theory, the π^-/π^+ ratio is predicted, depending on whether the photon field interacts with the charged particle currents or with the nucleon magnetic moments, as

$$\pi^-/\pi^+ = \left[1 - \frac{q_o}{M}(1 - \beta \cos\theta)\right]^{-2}$$

or

$$\pi^-/\pi^+ = \left[1 - \frac{\gamma + \gamma_n}{\gamma - \gamma_n}\ \frac{q_o}{M}\ (1 - \beta \cos\theta)\right]^{-2}$$

where q_o = total pion energy, in laboratory

M = nucleon rest mass

β = v/c for pion

θ = angle between photon beam and pion

γ_p, γ_n = magnetic moment of proton, neutron

= 2.87, -1.91 Bohr magnetons

The first formula predicts a value for the ratio which is, in general, higher than the experimental value of the ratio for energies less than 400 Mev. The second formula, over the same interval of energies, predicts a ratio less than the experimental value. Both correctly predict that the values of the ratio will increase with pion angle and photon energy.

At the energies with which this experiment is concerned, the photon wave length is becoming comparable to the dimensions of the circulating charges which cause the magnetic moments and of the nucleon charge distribution. Therefore, since the distribution of the nucleon charge must be considered, and since the static magnetic moments, which are used above, no longer have meaning, it is not surprising that these formulae no longer give valid qualitative predictions.

In the energy region below 400 Mev a good fit to the measured values of the ratio was made through a partial wave analysis (14). This fit, however, depended on the values of small terms from certain non-resonant angular momentum states. At higher energies, where many more non-resonant angular momentum states must be considered, this method of fitting the data becomes extremely tedious, and loses much physical significance. It seems unlikely that a simple explanation of the observed behavior of the π^-/π^+ ratios at high energies will be found in such an analysis.

E. Conclusions

The variations of the π^-/π^+ ratio have been successfully explored in the photon energy interval of 500 to 1000 Mev. Although the decrease of the ratio with increasing photon energy has not been explained, these measurements should help with the theoretical interpretation of photoproduction in this energy interval.

Until there is some theoretical reason for wishing to examine some particular part of the overall energy interval, or for obtaining more statistics, more effort on measuring the π^-/π^+ ratio would seem misguided.

VI. POSITIVE PION CROSS-SECTIONS FROM DEUTERIUM

A. Calculations

The yields of positive pions from deuterium will be used to calculate the ratio of the differential cross-sections for positive pion photoproduction from deuterium and hydrogen. Ideally, this ratio would be measured by comparing the counting rates from targets filled with deuterium and with hydrogen, and applying appropiate small corrections to the observed ratio of counting rates, as has been done to find the π^-/π^+ ratio. This course of action, however, was not practical. It was necessary to obtain the ratio of deuterium and hydrogen cross-sections by comparing the results of this experiment with those of a previous experiment on photoproduction from hydrogen (4). Although this latter experiment was performed with very nearly the same apparatus which has been used for the present experiment, it appeared more practical to calculate differential cross-sections from the deuterium data and compare them with the corresponding hydrogen cross-sections than to try to make a comparison of the counting rates of the two different experiments.

The differential cross-section from deuterium will be given by

$$\frac{d\sigma}{d\Omega'} = C^+ \left[\frac{W \rho N_o \bar{I} R A \varepsilon}{E_o M} \int \mathcal{R}(K) dK \right]^{-1}$$

A-1. Absorption

The absorption factor A, if determined correctly, would depend on the momentum of the pion considered. However, since the experiment from hydrogen used values for the absorption factor which were constant over the range of pion momenta considered,

the calculations for this experiment have used the same values. In this manner, although some error is introduced into the absolute cross-sections, the ratio of cross-sections for the two experiments will not include that error. The values of A which have been used are given below:

	A
Configuration I	.800 ± .030
Configuration II	.851 ± .023

The actual error introduced into the absolute cross-sections by neglecting the variation in the absorption with pion momentum is probably less than a few per cent.

A-2. Decay

A discussion of the calculation of the decay correction factor, R, will be found in the Appendix. The values of R which have been calculated for this experiment are shown in Table 10.

A-3. Efficiencies

Possible small inefficiencies in all of the counters, except the Cerenkov counter, have been neglected. The measurements which were made of the Cerenkov efficiency indicated that this efficiency varied by several per cent between 550 and 750 Mev/c. (See Figure 4) Calculations on the light output from the counter indicated that the photon flux from the counter should only be increased by 1.7 per cent between 600 Mev/c and 900 Mev/c. It seems unlikely that the measured variation in the efficiency of the counter can be accounted for by the variation in light output from the counter. If possible effects due to the small number of photoelectrons produced from the cathode of the phototube are neglected, it seems

reasonable to assume that the measurements, which were not made with a great deal of care, are not reliable. Additional evidence that the efficiency of the Cerenkov counter for counting pions should not vary with momentum was obtained by studying earlier measurements of the efficiency of the same counter (4). The value of the Cerenkov efficiency which has been used to calculate the cross-sections from deuterium is 97 per cent. This value represents a rough average of the present measurements and those measurements made earlier. Since none of the measurements upon which this estimate is based appear to be very reliable, an error as high as 2 per cent may have been introduced into the ratio of deuterium and hydrogen by this estimate.

A-4. Density, Beam Calibration

The calculations of the deuterium density have been discussed in Section III-F. The values of the density, effective target length, and total beam energy which have been used in the determination of the cross-sections from deuterium are shown in Table 5.

A-5. Pair Contamination

Measurements on the effects of contamination from pion pair production indicated that the π^-/π^+ ratio would be unaffected by any possible contamination at the bremsstrahlung endpoints selected for this experiment. These measurements did not, however, indicate with any certainty whether or not pions from pairs might contribute significantly to the absolute yields of positive pions.

At the bremsstrahlung limits used for this experiment, no pions which were multiply-produced from free target nucleons

Table 5. BEAM AND TARGET CONSTANTS

E_o = bremsstrahlung endpoint

U = beam energy per coulomb

W = energy in beam per BIP

= U x G, where G = $.2162 \pm .002 \times 10^{-6}$ coulombs/BIP

$\bar{l}$ = effective length of target

ρ = effective deuterium density

E_o (Mev)	U (10^{18} Mev/coul.)	W (10^{12} Mev/BIP)	$\bar{l}$ (cm)
600	4.48	.968	7.217
700	4.65	1.006	7.229
800	4.84	1.046	7.239
900	5.03	1.087	7.245
1000	5.19	1.122	7.236
1080	5.31	1.149	7.224

Configuration I	Configuration II
ρ = .1665 gm/cc	.1634 gm/cc

would have had enough energy to be counted by the spectrometer. The motion of the nucleons within the deuteron, however, changes this situation. Early calculations on the effects of the nucleon motion indicated that the production of multiply-produced pions of sufficient energy to pass through the spectrometer would be kinematically possible from as many as 10 per cent of the target nucleons. Therefore, some consideration must be given to the possibility of contamination from multiply-produced pions.

By extrapolating the results of the pion pair experiment of M. Bloch and M. Sands (15), an estimate may be made of the expected contribution to the counting rate from pion pairs. It is assumed that the contamination from positive pions from pairs will be comparable to the contamination from negative pions from pairs. This assumption, as has been shown by Sellen et al. (16), is not entirely correct. Further, it is assumed that pair production from neutrons is comparable to that from protons.

Bloch defines a quantity $\sigma^*_{T,\theta}(E_o)$ which is the yield per effective quantum of pions of kinetic energy T at an angle θ for a bremsstrahlung endpoint E_o. The counting rate is then given by:

$$C = Q\, n\, \eta\, \Delta\Omega\, \Delta T\, \sigma^*_{T,\theta}(E_o)$$

where n is the counting efficiency

η is the number of target nucleons/cm^2

$\Delta\Omega$ is the magnet solid angle

ΔT is the spread in pion kinetic energies accepted by the spectrometer

Q is W/E_o

The calculations on the effects of the nucleon motion within the deuteron have determined a quantity k*, which is the photon energy at which contamination from multiply-produced pions becomes kinematically possible. This quantity is a function of the actual momentum assigned to the target nucleon. At backward pion angles, k* was less than E_o for about 10 per cent of the target nucleons. The average of k* over all target nucleon momenta for which $k^* < E_o$ was taken. This quantity, $\bar{k}^*$, was as much as 100 Mev below E_o.

Bloch's data indicate the value of $\sigma^*_{T,\theta}(E_o)$ at 150 Mev, 120° is 0.05×10^{-32} cm^2/ster/Mev when E_o is 100 Mev above the kinematic limit for pair production. This pion angle and energy are very close to the values selected when the present experiment was run at backward pion angles. If it is assumed that the values of $\bar{k}^*$ which were determined from the nucleon motion are comparable to the kinematic limits for pair production from free nucleons, then Bloch's data may be used to estimate the contamination present in this experiment. The quantities used in this estimate are:

$$n = 0.85$$

$$\eta = \rho N_o \bar{T}$$

$$\Delta\Omega = .00603 \text{ ster.}$$

$$\Delta T < \Delta P \simeq 30 \text{ Mev}$$

$$Q \simeq 10^9/\text{BIP}$$

Since less than 10 per cent of the nucleons may contribute to the contamination, the value of the density which must be used is $\rho' < 0.1\rho_D = 0.1 \times .1634$ gm/cc.

The pion counting rate from pion pairs will be:

$$C < Q\, n\, 0.1\, N_o\, \bar{T}\, \rho_D \Delta T \Delta\Omega\, \sigma^*_{T,\theta}(E_o)$$

$$< 6 \times 10^{-3}/\text{BIP}$$

The observed counting rates are always greater than .200/BIP. Therefore, at backward angles, the contamination from pion pairs should be less than 3 per cent. At smaller pion angles the fraction of target nucleons from which sufficiently energetic pions from pairs can be produced is much smaller, and the values of $\bar{k}^*$ are much closer to E_o. For such angles, the contamination would be a small fraction of the figure given above. In all cases the contamination from pion pairs has been neglected in the calculation of the cross-sections from deuterium.

A-6. Cross-sections from Hydrogen

The cross-sections for positive pion production from hydrogen, which appear in Table 7, have been taken, with some modification, from the experiment of Dixon and Walker (4). The decay correction factors which were calculated for the present experiment did not seem to be in agreement with those used for the reduction of the hydrogen data, in spite of the fact that the methods used to calculate these factors appear to be similar. The calculations made for the hydrogen experiment made fewer approximations than did those used for this experiment and should, therefore, give a more accurate result. However, internal inconsistencies have appeared in the calculations of the decay factors which were used for the hydrogen experiment. Therefore, it has been assumed that they are wrong. Because

the difference in the two decay correction factors makes a difference of about 4 per cent in the values of the cross-sections, new calculations for the decay correction factor for the hydrogen experiment were made, and the cross-section modified accordingly. These modified cross-sections are the ones appearing in Table 7.

B. Results

The absolute cross-sections which have been calculated for the photoproduction of positive pions from deuterium are shown in Table 6. The values of $\int R(K)dK$ which were computed from the effects of the nucleon motion are also shown in this table.

The odd values of the effective photon energy at which this experiment was performed make a direct comparison with the results of the experiment from hydrogen somewhat difficult. The measured value of the cross-sections from deuterium were used to find interpolated (or extrapolated) values of the cross-section at 100 Mev intervals. These values are shown in Table 7, along with the corresponding cross-sections for hydrogen. All values shown for the photoproduction from hydrogen were measured directly, with the exception of the values at 40° center-of-mass, and the value at 100°, 1000 Mev. The values of the cross-section in these cases were obtained by interpolating between the nearest angles at which data were taken. All interpolations assumed that the cross-sections varied linearly between the values at those points at which data were taken.

Table 6. DIFFERENTIAL CROSS-SECTIONS FOR POSITIVE PIONS PRODUCED FROM DEUTERIUM

k = nominal photon energy in Mev

θ_{CM} = nominal center-of-mass pion angle in degrees

$\overline{K}$ = effective photon energy in Mev

C^+ = counting rate, in counts per BIP, of positive pions from deuterium

$H = \int R(K)dK$, in 10^{-3} ster.

$Y = \rho N_o \frac{\overline{I} W A \epsilon}{M E_o}$, in 10^{-32} cm^{-2} BIP^{-1}

R = decay correction factor

$\frac{d\sigma}{d\Omega}$ = differential cross-section for positive pion photoproduction from deuterium, in 10^{-30} cm^2/ster.

$H' = \int R(K)dK$ if target nucleons are assumed to be at rest. The value of H/H' indicates how large a correction has been made to correct the cross-sections for the motion of the nucleons within the deuteron.

k		θ_{CM}	$\bar{K}$	C^+	H	Y	R	$d\sigma/d\Omega'$	H/H^1
500	I	20	506	1.246±.046	.3404	4.497	.9315	8.74±.31	.994
	II	40	507	3.989±.135	.9833	4.840	.9639	8.70±.29	.989
		60	508	3.279±.110	.8739		.9586	8.08±.27	.974
		90	506	1.655±.066	.6833		.9448	5.30±.21	.936
		120	505	.634±.033	.5043		.9138	2.85±.14	.894
		150	498	.427±.027	.3740		.8819	2.67±.17	.866
		161	498	.385±.035	.3447		.8744	2.64±.24	.857
600	I	20	605	1.342±.049	.3803	4.013	.9430	9.33±.33	.996
	II	40	608	4.300±.160	1.065	4.319	.9666	9.67±.35	.986
		60	609	3.594±.138	.9487		.9625	9.12±.34	.964
		90	607	1.595±.062	.735		.9492	5.30±.20	.919
		120	599	.649±.032	.5237		.9262	3.09±.16	.857
		150	590	.328±.023	.3798		.8938	2.24±.14	.831
		162	588	.308±.028	.3475		.8829	2.33±.21	.822
700	I	20	704	1.350±.048	.4173	3.656	.9510	9.31±.26	.997
		40	704	1.358±.049	.3890		.9436	10.12±.36	.982
		60	706	1.021±.040	.3438		.9468	8.58±.33	.956
	II	60	708	3.734±.115	1.029	3.934	.9656	9.55±.29	.956
		90	704	1.939±.049	.7840		.9531	6.59±.16	.904
		120	699	.773±.025	.5364		.9316	3.93±.12	.828
		150	682	.315±.026	.3799		.9003	2.34±.19	.802
		162	677	.291±.028	.3413		.8893	2.44±.39	.795

k		θ_{CM}	$\overline{K}$	C^+	H	Y	R	$d\sigma/d\Omega'$	H/H^1
800	I	20	806	.979±.040	.4563	3.380	.9568	6.63±.27	.998
		40	804	.881±.040	.4203		.9521	6.51±.29	.977
		60	805	.705±.031	.3677		.9441	6.01±.26	.945
	II	90	801	1.237±.039	.822	3.637	.9565	4.33±.13	.883
		120	791	.620±.025	.5539		.9347	3.30±.13	.816
		150	769	.299±.021	.3799		.9052	2.39±.16	.798
		163	766	.188±.018	.3332		.8939	1.70±.16	.796
900	I	20	903	1.007±.035	.4929	3.136	.9600	6.78±.23	1.000
		40	904	.934±.045	.4510		.9565	6.91±.33	.971
		60	903	.557±.024	.3894		.9501	4.81±.21	.932
	II	90	899	.724±.033	.8523	3.375	.9607	2.62±.09	.862
		120	882	.502±.027	.5641		.9399	2.81±.10	.806
		150	861	.251±.018	.3680		.9205	2.19±.09	.794
		164	851	.187±.018	.3229		.9114	1.88±.09	.800
1000	I	20	1003	.758±.035	.5209	2.969	.9597	5.11±.23	.981
		40	1002	.940±.042	.4744		.9544	7.00±.31	.956
		60	1002	.564±.026	.4101		.9474	4.89±.22	.914
		85	952	.210±.015	.3284		.9362	2.30±.16	.92
	II	100	988	.455±.020	.7264	3.003	.9565	2.05±.09	.821
		120	972	.418±.020	.5358		.9435	2.59±.12	.808
		150	937	.240±.015	.3284		.9362	2.30±.16	.809
		164	928	.183±.015	.2999		.9047	2.11±.10	.827

Table 7. COMPARISON OF DIFFERENTIAL CROSS-SECTIONS FOR POSITIVE PIONS PRODUCED FROM DEUTERIUM AND HYDROGEN

$\overline{K}$ = effective photon energy in Mev

θ_{CM} = center-of-mass pion angle in degrees

$(\frac{d\sigma}{d\Omega'})_D$ = differential cross-section for photoproduction of positive pions from deuterium ($10^{-30} cm^2/ster.$)

$(\frac{d\sigma}{d\Omega'})_H$ = differential cross-section for photoproduction of positive pions from hydrogen ($10^{-30} cm^2/ster.$)

$\frac{(d\sigma/d\Omega')_D}{(d\sigma/d\Omega')_H}$ = ratio of differential cross-sections for photoproduction of positive pions from deuterium and hydrogen

$\bar{K}$	θ_{CM}	$(d\sigma/d\Omega')_D$	$(d\sigma/d\Omega')_H$	$\frac{(d\sigma/d\Omega')_D}{(d\sigma/d\Omega')_H}$
500	20	8.70±.31		
	40	8.63±.29		
	60	8.00±.27		
	90	5.30±.21	4.91±.35	1.079±.086
	120	2.85±.14		
	150	2.66±.17		
	161	2.63±.24		
600	20	9.30±.33	11.67±.71	.797±.056
	40	9.61±.35	10.80±.38	.890±.046
	60	9.02±.34	9.62±.35	.938±.048
	90	5.30±.20	5.88±.28	.901±.053
	120	3.09±.16	3.59±.17	.861±.060
	150	2.29±.14	2.68±.16	.854±.070
	162	2.34±.21	2.42±.19	.967±.115
700	20	9.31±.26	11.65±.62	.799±.050
	40	10.09±.36	10.36±.57	.974±.068
	60	9.16±.22	10.14±.20	.903±.029
	90	6.54±.16	8.09±.28	.808±.035
	120	3.94±.12	4.20±.20	.938±.053
	150	2.36±.19	2.63±.19	.897±.095
	162	2.26±.23	2.29±.19	.987±.132
800	20	6.79±.27	8.77±.44	.774±.050
	40	6.65±.29	7.06±.42	.942±.065
	60	6.16±.26	5.54±.18	1.112±.060
	90	4.34±.13	4.29±.14	1.012±.046
	120	3.25±.13	3.19±.16	1.019±.062
	150	2.33±.16	2.28±.15	1.022±.093
	163	1.79±.16	2.04±.16	.877±.097

$\bar{K}$	θ_{CM}	$(d\sigma/d\Omega')_D$	$(d\sigma/d\Omega')_H$	$\frac{(d\sigma/d\Omega')_D}{(d\sigma/d\Omega')_H}$
900	20	6.78±.23	8.05±.44	.842±.056
	40	6.89±.33	7.35±.47	.937±.073
	60	4.93±.21	4.73±.27	1.042±.071
	90	2.62±.09	2.49±.12	1.052±.061
	120	2.77±.10	2.54±.13	1.091±.064
	150	2.27±.11	2.09±.14	1.086±.075
	164	2.03±.10	2.07±.16	.981±.075
1000	20	5.16±.23	6.48±.37	.796±.057
	40	7.00±.31	9.25±.43	.757±.046
	60	4.89±.22	6.77±.40	.722±.054
	100	2.11±.10	2.19±.11	.963±.059
	120	2.50±.12	2.78±.11	.899±.060
	150	2.44±.11	2.54±.17	.961±.093
	164	2.33±.10	2.10±.18	1.110±.100

The differential cross-sections shown in Table 7 have been fitted, at each energy, to a polynomial in cos θ, up to powers of $\cos^4$. The total cross-sections have been determined by integrating the resulting polynomial. These total cross-sections and the ratios and differences of the total cross-sections for deuterium and hydrogen are shown in Table 8.

C. Errors

The errors which are listed with the cross-sections from deuterium and with the deuterium-hydrogen ratios are statistical counting errors. The absolute calibration of the equipment, the decay correction factor, the absorption of pions, and the counter inefficiencies all introduce small errors which have been neglected, since their effect on the ratio of deuterium and hydrogen cross-sections is insignificant in comparison to the statistical errors.

In addition to possible experimental difficulties, there are two major sources of possible error. The first of these is the nucleon motion within the deuteron. A few measurements were made to try to determine experimentally the accuracy of predictions based on the calculations of the effects of this motion (11). Although these measurements gave rough agreement with the predictions, they are not sufficient to confirm all of the assumptions which have been made in the calculations. The values of the cross-sections from deuterium which are listed are very dependent on these calculations, since they have been used to determine the effect of the bremsstrahlung cutoff on the counting rates. The values of $\int R(K)dK$ which have been used for the determination of the cross-sections from deuterium are as much as 20 per cent smaller than the values

Table 8. COMPARISON OF TOTAL CROSS-SECTIONS FOR POSITIVE PIONS PRODUCED FROM DEUTERIUM AND HYDROGEN

$\overline{K}$ = effective photon energy (Mev)

σ_D = total cross-section for positive pion photoproduction from deuterium (μb.)

σ_H = total cross-section for positive pion photoproduction from hydrogen (μ b.)

$\Delta\sigma = \sigma_H - \sigma_D$ (μb.)

$\overline{K}$	σ_D	σ_H	σ_D/σ_H	$\Delta\sigma$
500	68.5±1.2	72 ±4*	.95±.05	3.5 ±5
600	72.7±1.3	81.6±1.6	.891±.023	8.89±1.73
700	80.5±1.0	91.8±1.5	.877±.018	11.25±1.77
800	57.1±1.0	57.5±1.0	.992±.025	0.45±1.43
900	47.0±0.8	46.8±1.1	1.004±.029	-0.19±1.39
1000	44.7±0.9	55.8±1.4	.801±.026	11.12±1.71
1000**	43.1±1.0	53.3±1.7	.809±.032	10.17±1.97

* estimated

** fitted to $\cos^6$

which would have been used in the absence of nucleon motion.

The smearing effect of the nucleon motion spreads the equipment response over a wide interval of photon energies. In regions where the positive pion cross-section varies rapidly, as it does at small pion angles at high photon energies, this effect might lead to a difference between the cross-sections determined for deuterium and for hydrogen.

The second major possible cause of error is the interpolation which has been made to compare the hydrogen and deuterium cross-sections. The extrapolation of the measurements, which was necessary for part of the results at 1000 Mev, is even more likely to lead to error.

These possible sources of error make it appear that the actual errors in the values of the cross-sections from deuterium, and in the ratios of these cross-sections to the corresponding cross-sections from hydrogen, might be as much as twice the errors which are listed.

D. Discussion

Earlier experiments on the photoproduction of positive pions from deuterium have shown that the ratio of deuterium and hydrogen cross-sections, at lower energies, is somewhat less than unity (6). This experiment indicates that this is still the situation at photon energies up to 1000 Mev.

The Pauli exclusion principle, discussed in detail by Chew and Lewis (17), predicts a reduction in the cross-sections from deuterium for small pion angles. This effect becomes quite small at high energies, although it should still be noticeable for small

pion angles. Their predictions, for the case in which the nucleon spin flips during the production process and that in which it does not flip, are compared with the experimental values in Table 9. This comparison shows a rough qualitative agreement, since the ratios, at forward angles, do appear to be depressed about the order of magnitude which is predicted. In theory, it should be possible to determine with what probability the nucleon spin is changed during photoproduction by an examination of the experimental data. However, the scattering in the experimental data is too large to permit any conclusions. Also, the possibility that the deuteron as a whole becomes excited, which is not included in the predictions given in Table 9, causes, at the energies considered in this experiment, a greater reduction in the cross-section for most experimental settings than does the effect of the exclusion principle.

Earlier data taken at this laboratory, at lower photon energies (18), showed no effect of the exclusion principle at small pion angles (30° in laboratory).

At higher photon energies, the major cause of the difference between the cross-sections of pion photoproduction from deuterium and hydrogen is expected to be due to the possibility that the excitation of one of the nucleons of the deuteron will lead to the excitation of the deuteron as a whole. An estimate of the size of this effect may be made by using the known cross-sections for the elastic photodisintegration of the deuteron (19) and the phase space arguments given by Fermi (20).

Table 9. EFFECT OF PAULI EXCLUSION PRINCIPLE*

k = nominal photon energy (Mev)

θ_{CM} = center-of-mass pion angle (degrees)

$(d\sigma_d^+/d\sigma_h^+)_{sf}$ = predicted ratio of differential cross-sections from deuterium and hydrogen if nucleon spin flips

$(d\sigma_d^+/d\sigma_h^+)_{nf}$ = predicted ratio for no flip

$(d\sigma_d^+/d\sigma_h^+)_{exp.}$ = experimental value

k	θ_{CM}	$(d\sigma_d^+/d\sigma_h^+)_{sf}$	$(d\sigma_d^+/d\sigma_h^+)_{nf}$	$(d\sigma_d/d\sigma_h^+)_{exp.}$
500	90	.98	.92	1.08±.09
600	20	.89	.66	.80±.06
	40	.94	.82	.89±.05
	60	.97	.91	.94±.05
	90	.98	.95	.90±.05
700	20	.89	.68	.80±.05
	40	.95	.86	.97±.07
	60	.98	.93	.90±.03
800	20	.91	.72	.77±.05
	40	.97	.91	.94±.07
900	.20	.92	.77	.84±.06
	40	.97	.92	.94±.07
1000	20	.91	.78	.80±.06
	40	.98	.94	.76±.05

*shown only for those angles where predicted effect is more than 5 per cent from unity

If σ^t is the total cross-section for the production of all pions, and σ^+ is the total cross-section for the single production of positive pions, then, at the energies of this experiment

$$\sigma^+ \simeq 0.3\sigma^t$$

If F is the fraction of the time, as predicted by Fermi, that the excitation of the deuteron will lead to elastic photodisintegration, then

$$\sigma_p^+ - \sigma_D^+ = \Delta\sigma \simeq 0.3\sigma^{pd}/F,$$

where σ^{pd} is the total cross-section for elastic photodisintegration. The table below shows the comparison of these predictions and the experimental results. All cross-sections shown in the table are in micro-barns.

K(Mev)	F	σ^{pd}*	$0.3\sigma^{pd}/F$	$\Delta\sigma$ (exp.)
500	.52	7.0 ± 1.0	4.2 ± 0.6	3.5 ± 5.0
600	.41	6.0 ± 1.0	4.5 ± 0.6	8.9 ± 1.7
700	.31	3.4 ± 1.0	3.3 ± 1.0	11.3 ± 1.8
800	.24	2.1 ± 0.5	2.6 ± 0.6	0.5 ± 1.7
900	.18	1.0 ± 1.0	1.7 ± 1.7	-0.2 ± 1.7
1000	.14	-------	-------	10.2 ± 2.0

The agreement is only qualitative. However, in view of the fluctuations in the experimental values of $\Delta\sigma$ and of the approximations which have been made, a qualitative agreement is all that could have been hoped for.

The fluctuation in the experimental values of $\Delta\sigma$ at 1000

*These are the experimental values of the cross-section for elastic photodisintegration as measured by H. Myers (19).

Mev can probably be attributed to difficulties with the interpolation and extrapolation which were used to find the values of the cross-sections. There is some indication that there is a maximum in the values of $\Delta\sigma$ at 700 Mev, corresponding to the second resonance in pion production. However, the fluctuation in the experimental values of $\Delta\sigma$ makes it very difficult to draw any definite conclusions from this observation.

E. Conclusions

The measurements of positive pions photoproduced from deuterium indicate that the ratio of the differential cross-sections for the photoproduction of positive pions from deuterium averages about 0.95 of the corresponding cross-sections from hydrogen in the photon energy interval between 500 and 1000 Mev. The difference in the total cross-sections from hydrogen and deuterium is in qualitative agreement with calculations based on measurements of the cross-sections for the elastic photodisintegrations of the deuteron. The scattering in the experimental results and the approximations which have been necessary to calculate the cross-sections from the pion yields from deuterium make it very difficult to draw any precise conclusions.

APPENDIX

A fraction of the pions produced in the target decay before they can be detected, through the reaction

$$\pi \longrightarrow \mu + \nu + 33.9 \text{ Mev}$$

Some of the muons produced in this manner pass through the detecting system and are counted as pions while others, having the wrong momentum or direction, are not counted. Since the detecting system was not capable of differentiating muons from pions, a calculation must be made to find the number of decay muons which are counted. Previous treatments of the decay effects in pion photoproduction have been made by Walker et al. (1) and by Dixon(4).

A decay correction factor, R, may be defined which is equal to the ratio of the observed counting rate to the counting rate which would have been observed had no decay occurred. This factor R will consist of two components, R_π and R_μ. The first component is the fraction of the pions which do not decay before they can be detected:

$$R_\pi = e^{-t/T}$$

where: t = time of flight through the apparatus

$= S/\beta c$

S = distance from target to final counter

β = v/c of pions

T = mean lifetime of the pions

$$= \frac{25.6 \text{ m}\mu\text{s.}}{\sqrt{1 - \beta^2}}$$

The second component is the relative counting rate from

the muons which are produced. This is most easily treated by dividing it into two parts, $R_{\mu f}$ and $R_{\mu r}$. The first part, $R_{\mu f}$, is the relative muon counting rate from pions which decay before they pass through the spectrometer magnet. The second part, $R_{\mu r}$, is the relative muon counting rate from pions which decay after they have passed through the magnet. The division between the two effects is made, for convenience, halfway between the target and the final counter.

The exact calculation of $R_{\mu f}$ is quite difficult, since the small angle between the pion and muon trajectories, at the point of decay, leads to complications in finding the number of muons which can pass through the magnet aperture. An upper limit for $R_{\mu f}$ can be readily calculated if it is assumed that this angle is exactly zero. The calculation of this upper limit is discussed in the paragraphs below. Mr. F. P. Dixon (4) has calculated, for several cases, the ratio of the actual decay counting rate to this upper limit. He finds that this ratio varies smoothly with pion momenta. The exact values of the ratio are between 0.76 and 0.94 for the pion momenta used in this experiment.

When a pion of energy U decays, the resulting muon energies are spread with equal probability between

$$U_1 = \frac{U U_1^*}{mc^2} + \frac{P P_1^*}{m}$$

and

$$U_1 = \frac{U U_1^*}{mc^2} - \frac{P P_1^*}{m} \qquad (21)$$

where the subscripts refer to the muon and the asterisks refer to quantities measured in the rest system of the pion. The probability

of counting the decay muon, if the pion decays, will depend on the amount of overlap between the interval of muon energies accepted by the spectrometer and the interval of muon energies defined above. This interval of overlap will be designated as $\Delta U'$. If it is assumed that the pions are uniformly distributed as a function of momentum, then W(P), the probability that the muon will be counted if the pion decays, may be written, in the upper limit approximation:

$$W(P) = m\,\Delta U'/2PP_I^*$$

This probability is plotted as a function of the pion momentum for a typical setting of the spectrometer in Figure 14. For production of pions from free nucleons, no pions will be produced of momentum higher than that momentum defined by E_o, the bremsstrahlung endpoint. The counting rate from muons will be given by

$$C_\mu = D(1-e^{-t/2T}) \int W(P)dP$$

where D is a constant, and $(1-e^{-t/2T})$ is the fraction of the pions which decay at the front of the magnet. If no decays occurred, the counting rate from pions would be given by

$$C_\pi = D\,A\,f \int W'(P)dP$$

where: A is the fraction of pions not absorbed before they are counted

$W'(P)$ is the probability of counting pions if no decay occurred

$W'(P) = 1.0$ for $(P_o - \frac{\Delta P}{2}) \leq P \leq (P_o + \frac{\Delta P}{2})$

$= 0$ everywhere else

Figure 14. EFFECT OF DECAY AT FRONT OF MAGNET

W(P) is the probability that a muon is counted if a pion of momentum P decays, provided that the angle between the muon and the pion trajectories, at the point of decay, is zero. The curve drawn represents the decay effects at the spectrometer setting corresponding to k = 700 Mev, $\theta_{CM} = 40^{o}$. P_o in this case is 672 Mev/c, and E_o is 800 Mev. The decay curves at other settings are similar, differing mainly in the position of $P(E_o)$.

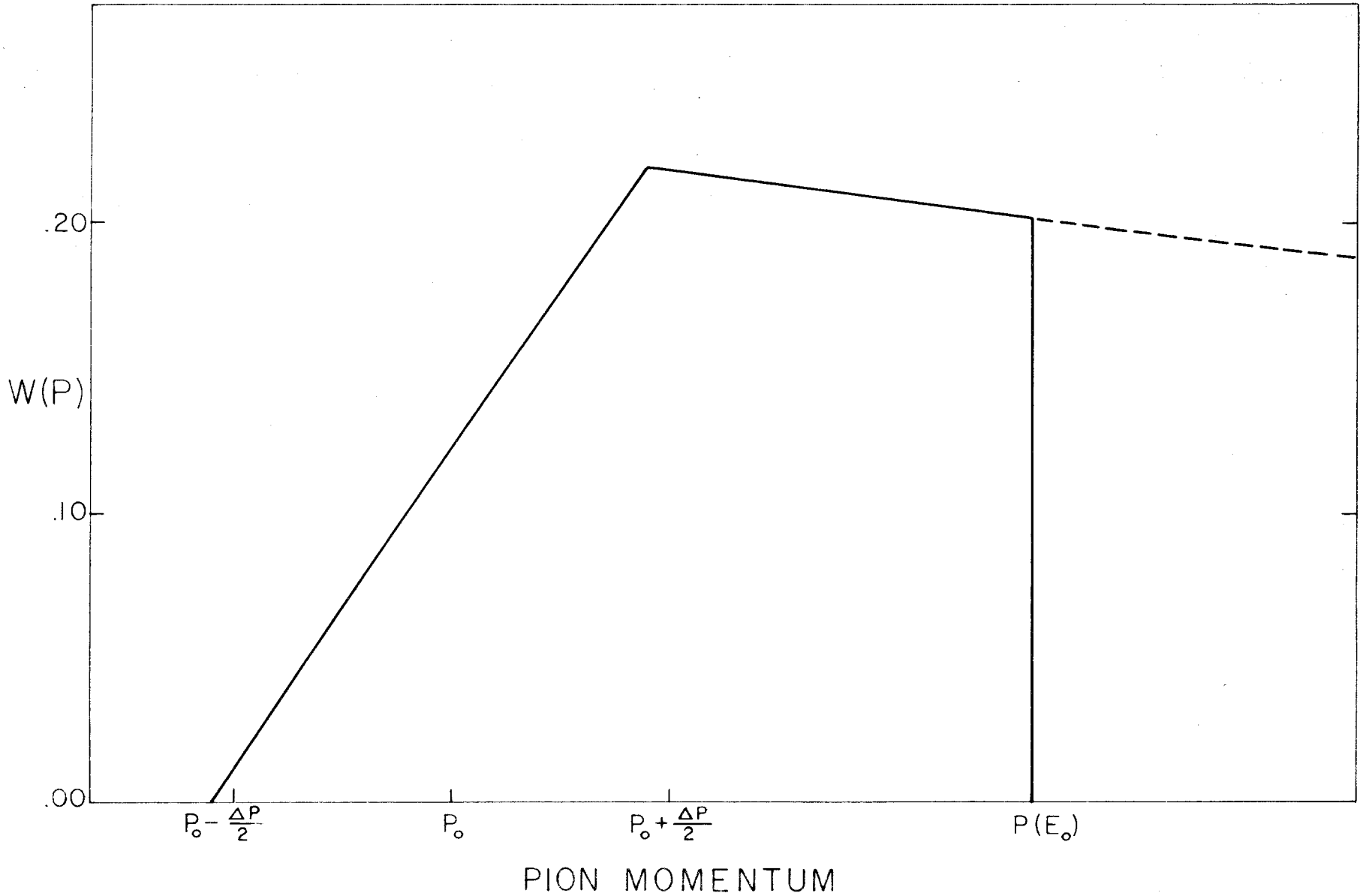
.20
.10
.00
W(P)
$P_o - \frac{\Delta P}{2}$
P_o
$P_o + \frac{\Delta P}{2}$
$P(E_o)$
PION MOMENTUM

P_o is the central momentum accepted by the spectrometer

ΔP is the momentum aperture of the spectrometer

$\Delta P \simeq 0.1 P_o$

f is a factor, usually near unity, which measures the effect of E_o in reducing the momentum aperture available to pions

$$f = \frac{\int_o^{E_o} \frac{d\Omega'}{d\Omega} \Delta\Omega(P) \frac{dk}{k}}{\int_o^{\infty} \frac{d\Omega'}{d\Omega} \Delta\Omega(P) \frac{dk}{k}}$$

The upper limit for the relative muon counting rate from pions which decay at the front of the magnet will be given by the ratio of these two counting rates:

$$R_{\mu f}(u.l.) = \frac{(1-e^{-t/2T}) \int W(P)dP}{A\ f \int W'(P)dP}$$

This quantity, when multiplied by the ratio computed by Dixon, yields the correct value of the relative counting rate from muons produced at the front of the magnet.

At the rear of the magnet, $(1-e^{-t/2T})e^{-t/2T}$ of the original pions decay. If the muons followed the same trajectories as the pions, all of the muons from pions which would have entered the counter system would be counted. However, the small angle between the muon and pion trajectories necessitates a calculation to find the number of muons which are counted.

In the figure below, a coordinate system has been set up on the defining counter S_2. If it is assumed that the pion momenta

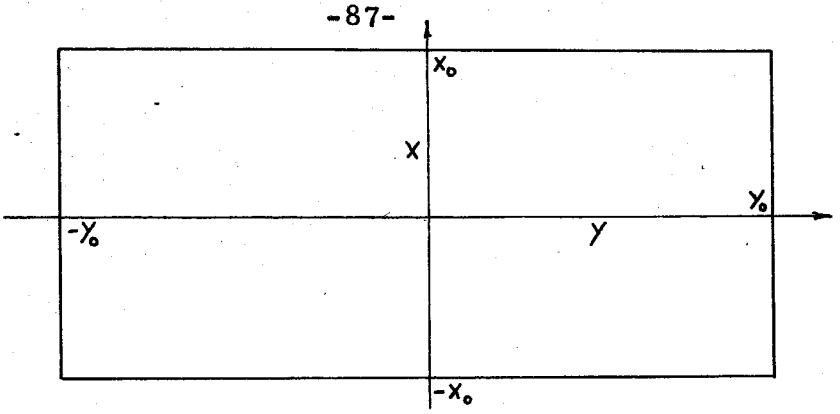

are distributed linearly in x, with pions of momentum $(P_o + \frac{\Delta P}{2})$ hitting the counter at x_o and pions of momentum $(P_o - \frac{\Delta P}{2})$ hitting at $-x_o$, then the probability that the decay muons hit the region between $-x_o$ and $+x_o$ can be determined as a function of the initial pion momentum. The results of such a determination, for a typical setting of the spectrometer, are shown in Figure 15. W(P) in the figure is the probability that the decay muon from a pion of momentum P will strike within the x limits of the counter.

The probability that the decay muon will strike between $-y_o$ and $+y_o$ may be determined as a function of y, where y is the point at which the pion would have hit if it had not decayed. This probability, W(y), is shown, for a typical setting of the spectrometer, in Figure 16. If g(y) is the actual distribution of pions over the counter, then the counting rate from muons is given by

$$C_\mu = D\,(1-e^{-t/2T})e^{-t/2T} \int W(y)\, g(y)\, W(P) dP dy$$

In practice, the integral has been done by integrating

$$\int W(y)\, g(y)\, dy \quad \int W(P) dP$$

on the assumption that the integral over one probability may be done independently of the other. This approximation results in a great deal of simplification. A careful analysis of the effects of

Figure 15. EFFECT OF DECAY AT REAR OF MAGNET - VERTICAL

W(P) is the probability that a muon lands within the vertical limits of the counter if a pion decays, as a function of the pion momentum P. The curve drawn represents the decay effects at k = 700 Mev, $\theta_{CM} = 40^{\circ}$. Curves for other points differ somewhat in the exact shape and in the position of the cutoff at $P(E_o)$.

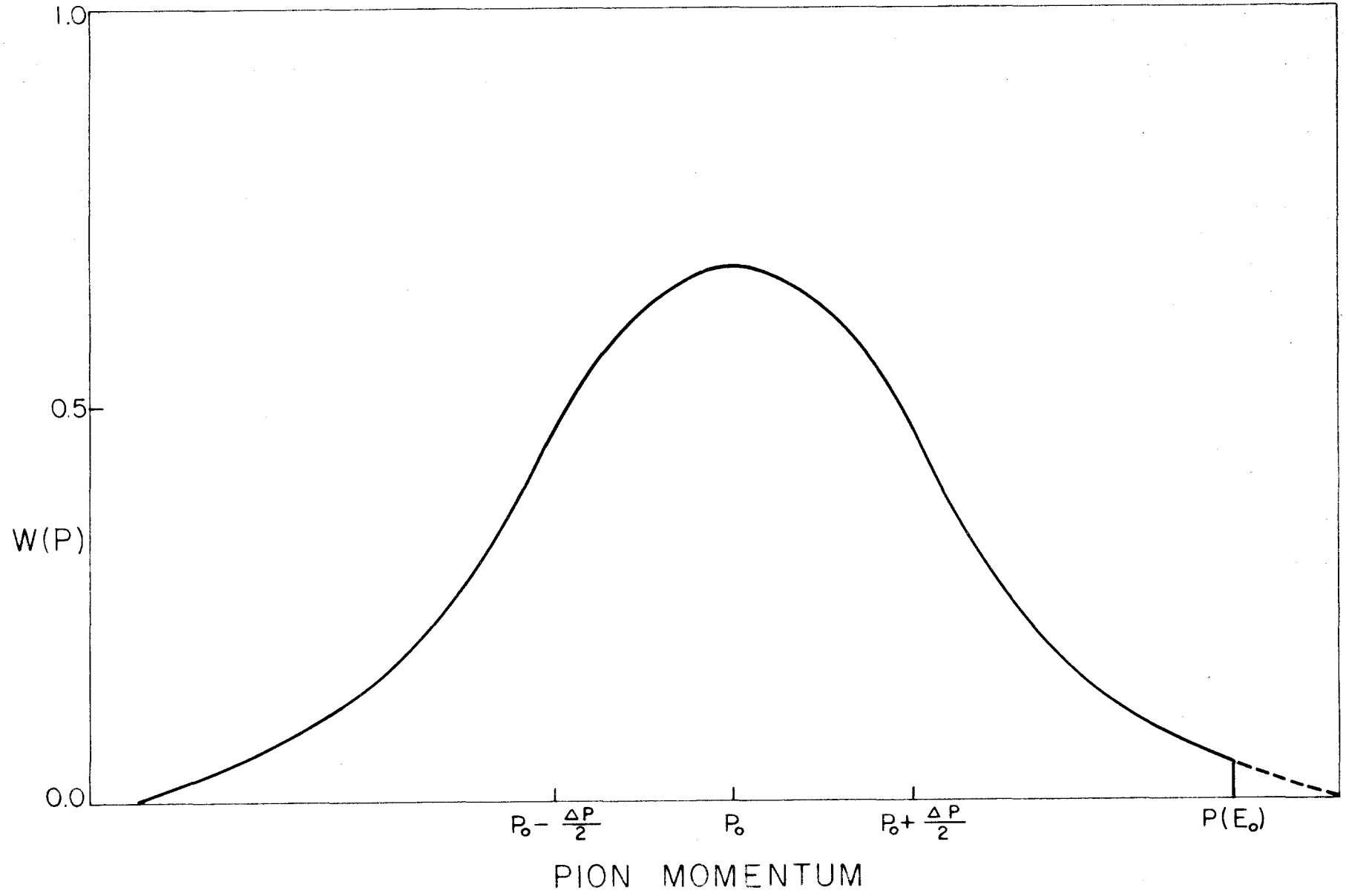
1.0
0.5
0.0
W(P)
$P_o - \frac{\Delta P}{2}$
P_o
$P_o + \frac{\Delta P}{2}$
$P(E_o)$
PION MOMENTUM

Figure 16. EFFECT OF DECAY AT REAR OF MAGNET - HORIZONTAL

W(y) is the probability that the muon lands within the horizontal limits of the counter if the pion decays, as a function of the horizontal position at which the pion would have struck the counter. This curve is drawn for a pion momentum of 672 Mev/c. Curves for other momenta are similar.

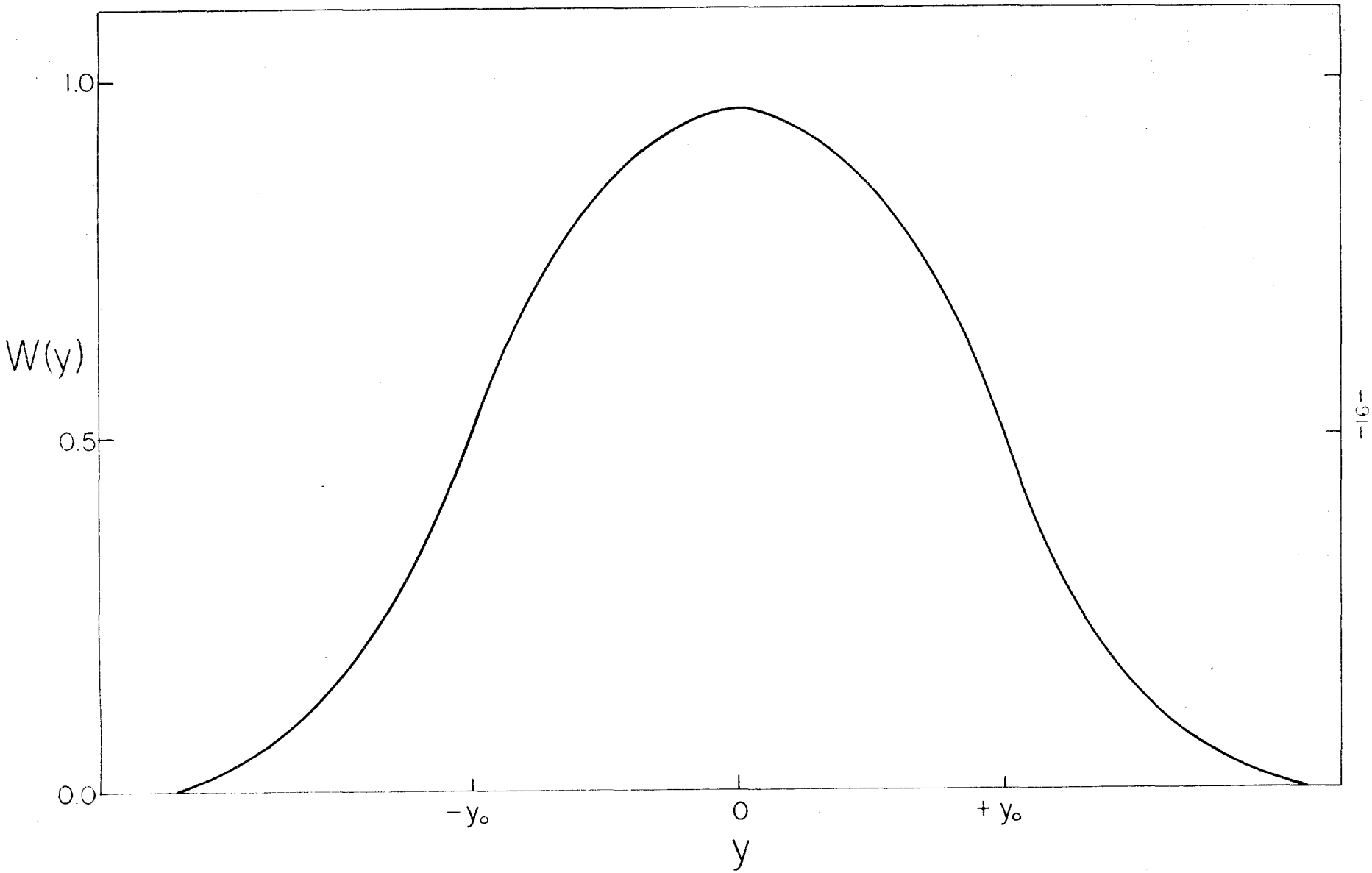
1.0
0.5
0.0
W(y)
−y₀
0
+y₀
y

this approximation indicates that it will never introduce an error larger than 5 per cent, and will seldom introduce errors as large as 2 per cent.

The counting rate for pions, if no decays occurred, would be

$$C_\pi = D\,A\,f \int W'(y)\, g(y)\, dy \int W'(P) dP$$

where $W'(y)$ is equal to unity. The absorption factor is somewhat different than the one used with the decays at the front of the magnet, since pions, once through the magnet, are less likely to be absorbed before they can be counted than are pions at the target.

The ratio of these two counting rates gives the decay correction at the rear of the magnet:

$$R_{\mu r} = \frac{(1-e^{-t/2T})e^{-t/2T} \int W(y)g(y)dy \int W(P)dP}{A\ f \int W'(y)g(y)dy \int W'(P)dP}$$

The motion of the nucleons within the deuteron makes the decay factor which is calculated in an experiment from deuterium somewhat different than that which would be calculated if the nucleons were assumed to be at rest. The motion of the nucleons tends to smear the sharp bremsstrahlung cutoff on W(P), as is shown in Figure 17. The integral of W(P) over the pion momentum is, in general, somewhat different from the integral which would have been calculated had the nucleons been assumed at rest.

The factor f, which measures the effect of E_o in reducing the momentum aperture available to pions, becomes

Figure 17. EFFECT OF DEUTERIUM SMEARING ON DECAYS AT FRONT OF MAGNET

W(P) is the probability that the muon is counted if the pion decays, as a function of the pion momentum. This curve corresponds to the spectrometer settings at k = 700 Mev, $\theta_{CM} = 40^{o}$. This curve should be compared with Figure 14, which is drawn for the case of production from free nucleons. A similar smearing of the sharp cutoff of W(P) at $P(E_o)$ is found in the decay effect at the rear of the magnet.

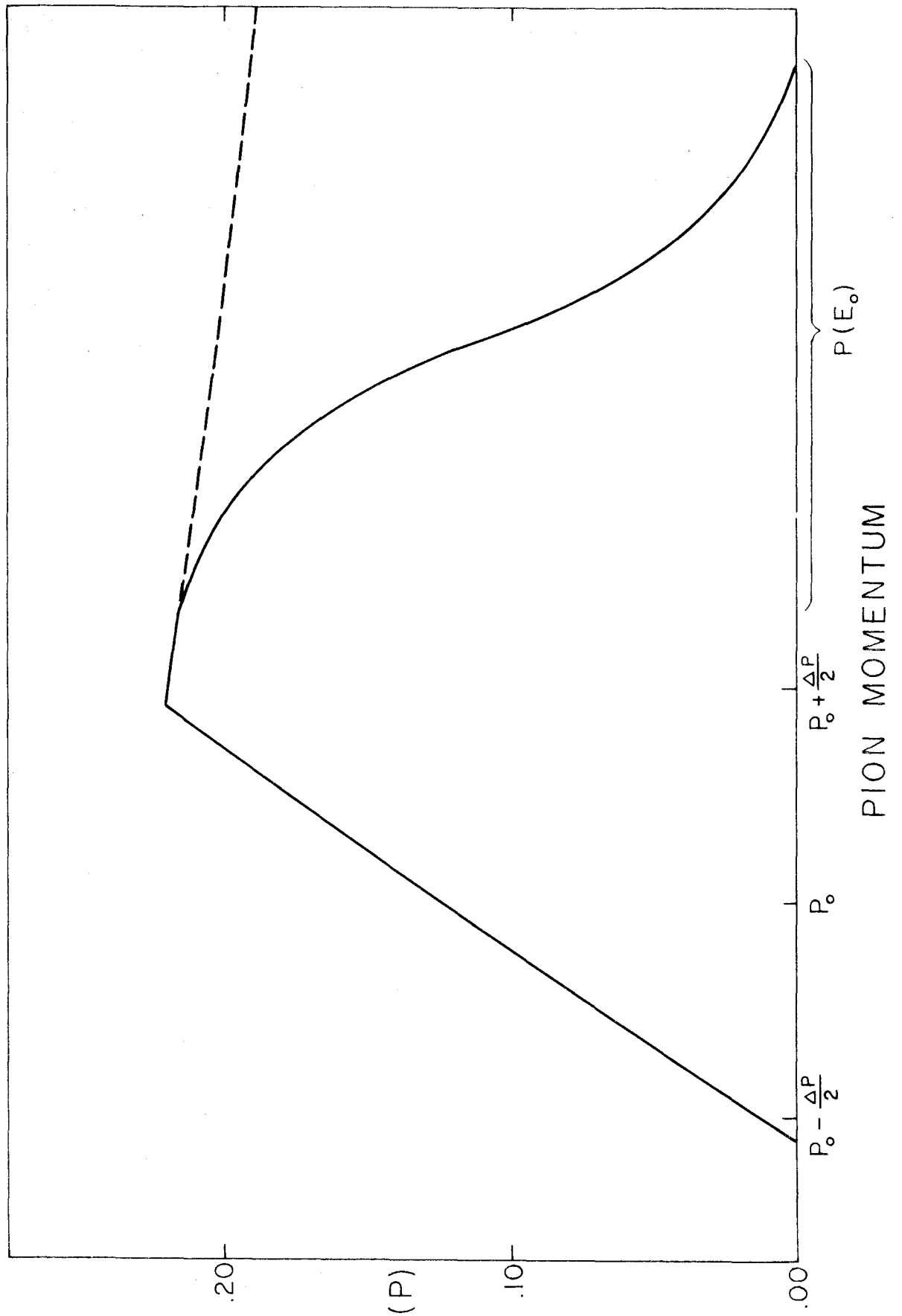
.20
.10
.00
W(P)
$P_o - \frac{\Delta P}{2}$
P_o
$P_o + \frac{\Delta P}{2}$
$P(E_o)$
PION MOMENTUM

$$f = \frac{\int \left[\sum_{E_o} \frac{d\Omega'}{d\Omega} \quad \frac{\Delta\Omega(P)}{k} \quad \frac{dk}{dK} \right] dK}{\int \left[\sum_{\infty} \frac{d\Omega'}{d\Omega} \quad \frac{\Delta\Omega(P)}{k} \quad \frac{dk}{dK} \right] dK}$$

The sums are taken over the momentum distribution of the target nucleons. The summation in the numerator of the expression above excludes those target nucleon momenta for which $k > E_o$, while the summation in the denominator includes all possible target nucleon momenta.

The values of the decay factor, R, have been calculated for all the experimental setting. A list of the calculated decay factors, and a few of the important quantities used in their determination, appears as Table 10.

To the first approximation, there is no correction to the π^-/π^+ ratio due to pion decays, since the actual value of R_μ will be exactly the same for positive and negative pions. The second order effects of the pion decay on the π^-/π^+ ratio may be estimated by considering the fact that both of the decay distributions shown in Figures 14 and 15 are offset somewhat from the central pion momentum accepted by the spectrometer. For decays at the front of the magnet, the center of the decay distribution is at some pion momentum corresponding to a photon energy of $k_o + a_f$, where k_o is the photon energy corresponding to the central pion momentum. At the rear of the magnet the distribution is centered at $k_o - a_r$. The quantities a_f and a_r are always positive.

The change in the observed ratio due to pion decay may be estimated by setting

Table 10. DECAY CORRECTION FACTORS

k = nominal photon energy (Mev)

θ_{CM} = pion center-of-mass angle (degrees)

$\overline{K}$ = effective photon energy (Mev)

f = reduction of momentum aperture for pions

A_f = fraction of pions not absorbed between front of magnet and final counter

$R_{\mu f}(u.l.)$ = upper limit of relative muon counting rate from decays at front of magnet

D = ratio of actual muon counting rate at front of magnet to upper limit

$R_{\mu f}$ = relative muon counting rate from decays at front of magnet

A_r = fraction of pions not absorbed between rear of magnet and final counter

$R_{\mu r}$ = relative muon counting rate from decays at rear of magnet

R_μ = relative muon counting rate from pion decay

$= R_{\mu f} + R_{\mu r}$

R_π = fraction of pions which do not decay

R = decay correction factor

$= R_\mu + R_\pi$

k	θ	$\overline{K}$	f	A_f	$R_{\mu f}$(u.l.)	D	$R_{\mu f}$
500	20	507	.994	.802	.0693	.76	.0527
	40	507	.990	.853	.0433	.906	.0392
	60	508	.974		.0452	.897	.0405
	90	506	.936		.0510	.876	.0447
	120	505	.894		.0577	.852	.0492
	150	498	.866		.0715	.832	.0595
	161	498	.857		.0752	.828	.0623
600	20	605	.996	.802	.0488	.83	.0405
	40	608	.986	.853	.0290	.925	.0268
	60	609	.964		.0309	.918	.0264
	90	607	.919		.0352	.897	.0316
	120	599	.857		.0428	.870	.0372
	150	590	.831		.0556	.844	.0469
	162	588	.822		.0586	.838	.0491

k	θ	A_r	$R_{\mu r}$	R_μ	R_π	R
500	20	.808	.1042	.1569	.7745	.9314
	40	.859	.0805	.1197	.8442	.9639
	60		.0852	.1257	.8329	.9586
	90		.0948	.1395	.8053	.9448
	120		.0979	.1471	.7667	.9138
	150		.0994	.1589	.7230	.8819
	161		.0995	.1619	.7126	.8744
600	20	.808	.0922	.1327	.8103	.9430
	40	.859	.0704	.0972	.8694	.9666
	60		.0753	.1037	.8588	.9625
	90		.0847	.1163	.8329	.9492
	120		.0937	.1309	.7953	.9262
	150		.0969	.1438	.7500	.8938
	162		.0967	.1458	.7371	.8829

k	θ	$\overline{K}$	f	A_f	$R_{\mu f}(u_o l_o)$	D	$R_{\mu f}$
900	20	903	1.000	.802	.0217	.940	.0204
	40	904	.971		.0224	.937	.0210
	60	903	.932		.0242	.917	.0222
	90	899	.858	.853	.0169	.928	.0157
	120	882	.786		.0223	.905	.0202
	150	861	.692		.0328	.870	.0285
	164	851	.664		.0384	.859	.0330
1000	20	1003	.980	.802	.0147	.940	.0138
	40	1002	.956		.0146	.940	.0137
	60	1002	.914		.0163	.937	.0153
	85	952	.952		.0254	.875	.0222
	100	988	.765	.853	.0141	.928	.0131
	120	972	.711		.0171	.914	.0156
	150	937	.675		.0272	.876	.0238
	164	928	.655		.0301	.864	.0260

k	θ	A_r	$R_{\mu r}$	R_μ	R_π	R
900	20	.808	.0690	.0894	.8706	.9600
	40		.0721	.0931	.8634	.9565
	60		.0775	.0996	.8504	.9501
	90	.859	.0653	.0810	.8797	.9607
	120		.0771	.0973	.8426	.9399
	150		.0961	.1246	.7959	.9205
	164		.1002	.1332	.7782	.9114
1000	20	.808	.0628	.0766	.8831	.9597
	40		.0645	.0782	.8762	.9544
	60		.0682	.0835	.8639	.9474
	85		.0830	.1052	.8312	.9362
	100	.859	.0640	.0771	.8794	.9565
	120		.0745	.0901	.8534	.9435
	150		.0885	.1123	.8048	.9170
	164		.0925	.1185	.7862	.9047

$N\underline{+}$ = real pion counting rate at k_o

$N\underline{+}^{a}$ = rate at $k_o + a$

$\overline{N}\underline{+}$ = observed counting rate

Then: $$\overline{N}\underline{+} = R_\pi N\underline{+} + R_{\mu f} N\underline{+}^{a_f} + R_{\mu r} N\underline{+}^{a_r}$$

Let $$N\underline{+}^{a} = N\underline{+} + a\, dN\underline{+}/dk$$

$$\overline{N}\underline{+} = R_\pi N\underline{+} + R_\mu N\underline{+} + (R_{\mu f} a_f - R_{\mu r} a_r) dN\underline{+}/dk$$

$$N\underline{+} = \frac{\overline{N}\underline{+} - (R_{\mu f} a_f - R_{\mu r} a_r) dN\underline{+}/dk}{R_\pi + R_\mu}$$

If $N_-/N_+ = r$, and $\overline{N}_-/\overline{N}_+ = \overline{r}$, then

$$r = \frac{\overline{N}_- - (R_{\mu f} a_f - R_{\mu r} a_r)\, dN_-/dk}{\overline{N}_+ - (R_{\mu f} a_f - R_{\mu r} a_r)\, dN_+/dk}$$

$$\simeq \overline{r} \left[1 + (R_{\mu f} a_f - R_{\mu r} a_r) \left(\frac{dN_+/dk}{N_+} - \frac{dN_-/dk}{N_-} \right) \right]$$

$$\Delta r = r - \overline{r} \simeq (R_{\mu f} a_f - R_{\mu r} a_r) \left[\frac{1}{\overline{N}_+^2} \left(\overline{N}_- \frac{dN_+}{dk} - \overline{N}_+ \frac{dN_-}{dk} \right) \right]$$

An evaluation of the quantity in brackets indicates that it can be, at most, somewhat less than .003/Mev. Since a_r and a_f are both positive, the absolute value of $(R_{\mu f} a_f - R_{\mu r} a_r)$ must be less than the value of the larger term. The maximum value of $R_\mu a$ for this experiment is never larger than 3.5 Mev. Thus, the maximum value of Δr must be less than .011. In general, the decay effects will be much less than this. This

effect has been regarded as insignificant in comparison to other sources of error, and has been completely neglected in computing the ratios of negative to positive cross-sections for pion photoproduction from deuterium.

REFERENCES

1. For example:

   Tollestrup, Keck, and Worlock, Phys. Rev. 99, 220 (1955)

   Walker, Teasdale, Peterson and Vette, Phys. Rev. 99, 210 (1955)

2. For example:

   Oakley and Walker, Phys. Rev. 97, 1283 (1955)

3. For example:

   J. I. Vette, Phys. Rev. 111, 622 (1958)

4. For example:

   Dixon and Walker, Phys. Rev. Letters, 1, 142, 458 (1958)

   F. P. Dixon, Ph. D. Thesis (unpublished)

5. Keck, Tollestrup, and Bingham, Phys. Rev. 103, 1549 (1956)

6. Lebore, Feld, Frisch, and Osborne, Phys. Rev. 85, 681 (1952)

   Littauer and D. Walker, Phys. Rev. 86, 838 (1952)

   White, Jacobson, and Schulz, Phys. Rev. 88, 836 (1952)

   Jenkins, Lucky, Palfrey, and Wilson, Phys. Rev. 95, 179 (1954)

   Sands, Teasdale, and Walker, Phys. Rev. 95, 592 (1954)

   with M. Bloch (unpublished)

   Hagerman, Crowe, and Friedman, Phys. Rev. 106, 818 (1957)

   Beneventano, Bernardini, Stoppini, and Tau, Nuovo Cimento 10, 1109 (1958)

7. R. Gomez, private communication

8. P. L. Donoho, "A Magnetic Spectrometer for Analysis of Charged Particles at Momenta Up to 1200 Mev/c" (unpublished)

9. H. Brody, Ph.D. Thesis (unpublished)

10. J. of Res. of NBS 41, RP 1932 (1948)

11. G. Neugebauer, Ph. D. Thesis (unpublished)

12. K. M. Watson, "On the Interpretation of Photomeson Production" - notes on lectures given at Caltech, 1954 (unpublished)

13. Bruckner and Goldberger, Phys. Rev. 76, 1725 (1949)
K. Bruckner, Phys. Rev. 79, 641 (1950)

14. Watson, Keck, Tollestrup, and Walker, Phys. Rev. 101, 1159 (1956)

15. Bloch and Sands, Phys. Rev. 113, 305 (1959)

16. Sellen, Cocconi, Cocconi, and Hart, Phys. Rev. 113 1323 (1959)

17. Chew and Lewis, Phys. Rev. 84, 779 (1951)

18. Teasdale, Sands, and Walker (unpublished)

19. H. Myers, Ph. D. Thesis (unpublished)

20. E. Fermi, Prog. Theor. Phys., 5, 570 (1950)

21. B. Rossi, "High Energy Particles", page 191, Prentice-Hall, Inc. (1952)